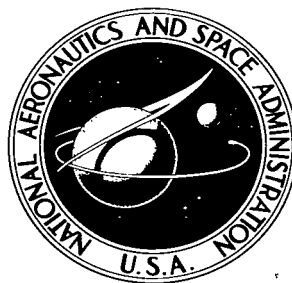


NASA TECHNICAL NOTE



NASA TN D-3619

c. 1



TECH LIBRARY KAFB, NM

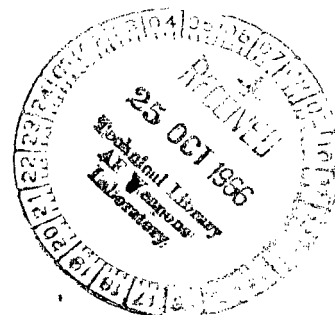
NASA TN D-3619

EVALUATION OF SEVERAL
SILICONE, PHENOLIC, AND EPOXY
BASE HEAT-SHIELD MATERIALS
AT VARIOUS HEAT-TRANSFER
RATES AND DYNAMIC PRESSURES

by Andrew J. Chapman

Langley Research Center

Langley Station, Hampton, Va.





EVALUATION OF SEVERAL SILICONE, PHENOLIC, AND EPOXY BASE
HEAT-SHIELD MATERIALS AT VARIOUS HEAT-TRANSFER RATES
AND DYNAMIC PRESSURES

By Andrew J. Chapman

Langley Research Center
Langley Station, Hampton, Va.

NATIONAL AERONAUTICS AND SPACE ADMINISTRATION

For sale by the Clearinghouse for Federal Scientific and Technical Information
Springfield, Virginia 22151 - Price \$2.50

EVALUATION OF SEVERAL SILICONE, PHENOLIC, AND EPOXY BASE HEAT-SHIELD MATERIALS AT VARIOUS HEAT-TRANSFER RATES AND DYNAMIC PRESSURES

By Andrew J. Chapman
Langley Research Center

SUMMARY

Three elastomeric ablative materials with a silicone resin base and three rigid ablators with an epoxy or phenolic resin base were tested in an electric-arc-heated gas stream. The materials were reinforced with a phenolic-glass-fiber honeycomb matrix. Seventy-one specimens, fabricated as 3-in-diameter (76 mm) flat-face disks, were exposed to a range of test stream conditions which included stagnation enthalpy from 1850 to 3370 Btu/lbm (4.3 to 7.8 MJ/kg), dynamic pressure from nearly 0 to 1000 lbf/ft² (48 kN/m²), and heat-transfer rate from 20 to 220 Btu/ft²-sec (0.23 to 2.5 MW/m²). A test stream of reduced oxygen concentration (3 percent oxygen and approximately 97 percent nitrogen) was used to simulate oxidation conditions in air at high enthalpy. The results presented include back-surface temperature response, thickness of degraded and undegraded layers after testing, and photographs showing conditions of the materials after testing. The thermal shielding performance of the materials is compared. Silicone resin base elastomeric materials produced the highest performance in a range of conditions where heating rate was less than 100 Btu/ft²-sec (1.14 MW/m²) and dynamic pressure was less than 50 lbf/ft² (2.4 kN/m²). In a range of conditions where heating rate was greater than 150 Btu/ft²-sec (1.7 MW/m²) and dynamic pressure was greater than 155 lbf/ft² (7.4 kN/m²) a more rigid epoxy base material produced superior performance, whereas the performance of the elastomeric materials deteriorated.

INTRODUCTION

An effective and practical method for reducing aerodynamic heating to the substructure of a spacecraft entering a planetary atmosphere is the use of a charring ablative coating on the heated surfaces. Such materials dissipate heat by simultaneous processes of ablation and reradiation. A continuing series of investigations has been in progress to further the understanding and to improve the performance of charring ablators. Among these investigations are references 1 and 2 which report the effect of varying composition

and density in a typical class of charring ablators and references 3 to 7 which report investigations of several materials at various environmental conditions.

The study of the effect of varying certain environmental parameters on the performance of charring ablators was continued in the present investigation. Two classes of charring ablators were considered: elastomeric formulations with a silicone resin base and more rigid formulations with a phenolic or epoxy resin base. A detailed investigation of a typical material in each of these classes is reported in reference 3. It was desired, however, to obtain performance data on several commercially available materials in each class which were under consideration for the heat shield for a manned reentry vehicle. The elastomeric material investigated in reference 3 and a Langley elastomeric formulation are also included in this investigation.

A test environment was produced by an electric-arc-heated gas stream composed of approximately 97 percent nitrogen and 3 percent oxygen. The range of nominal stream conditions included stagnation enthalpy from 1850 to 3370 Btu/lbm (4.3 to 7.8 MJ/kg), heat-transfer rate from 20 to 220 Btu/ft²-sec (0.23 to 2.5 MW/m²), and dynamic pressure from nearly 0 to 1000 lbf/ft² (48 kN/m²).

SYMBOLS

The units used for the physical quantities defined in this paper are given both in the U.S. Customary Units and in the International System of Units (SI) (ref. 8). The appendix presents factors relating these two systems of units.

A	area, feet ² (meters ²)
C	oxygen concentration
c _p	specific heat at constant pressure, British thermal units per pound mass-°R (joules per kilogram-°K)
d	diameter, feet (meters)
E	shielding effectiveness, British thermal units per pound mass (joules per kilogram)
F _c	compressibility factor
h	enthalpy, British thermal units per pound mass (joules per kilogram)

\dot{m}	mass flow rate, pounds mass per second (kilograms per second)
p	pressure, pounds force per foot ² (newtons per meter ²)
Q	cold-wall heat load, British thermal units per foot ² (joules per meter ²)
q_{∞}	dynamic pressure, pounds force per foot ² (newtons per meter ²)
\dot{q}	cold-wall stagnation-point heat-transfer rate (British thermal units per foot ² -second (watts per meter ²))
T	temperature, °R (°K)
ΔT	back-surface sensor temperature rise, °R (°K)
t	time, seconds
U	velocity, feet per second (meters per second)
w	mass distribution (unit mass) of test material, pounds mass per foot ² (kilograms per meter ²)
x	thickness of layers or distance from original front surface (see fig. 8)
ρ	density, pounds mass per foot ³ (kilograms per meter ³)

Subscripts:

A	atmospheric
a	char surface position
c	char layer
e	external to boundary layer
f	termination of exposure
i	undegraded layer

m	maximum
o	initial value
p	char-undegraded layer interface position
s	stagnation or front surface
t	total or arc chamber
ΔT	temperature rise
w	wall
∞	free stream
1,2	stream conditions

HEAT-SHIELD SPECIMENS

Heat-Shield Materials

Six materials were tested in this investigation. Five of the materials were products of companies which have been active in the design of thermal protection systems while the remaining material was fabricated at the Langley Research Center. Three of the materials had a silicone resin base and are elastomeric. The other materials had either a phenolic or epoxy resin base and are more rigid in nature than the elastomeric materials.

The materials are identified in table I by a code designation which is used hereafter throughout the paper. Known components are given for each material; however, the exact composition of the commercial materials was not available and the composition may vary from the information given in table I. The exact composition is given only for the Langley Research Center material E-1. All the materials were reinforced by a phenolic-glass-fiber honeycomb matrix. The honeycomb material had 3/16- to 1/4-in. (4.76 to 6.35 mm) hexagonal cells and a density of 4 to 9 lbm/ft³ (64 to 144 kg/m³).

Specimen Configuration and Instrumentation

Seventy-one ablative specimens were tested in this program. These specimens were 3-in-diameter (76 mm) disks with the thickness varied to give the mass per unit area for the particular test condition. The specimen assembly consisted of the test

material with a brass mounting ring and copper sensor bonded to the back surface as shown in figure 1. The back-surface sensor consisted of a 0.0625- or 0.125-in-thick (1.6 or 3.2 mm) copper calorimeter and concentric guard ring with the thermocouples attached at the center of the back surface of the calorimeter. The temperature monitored at the center of the calorimeter is hereafter referred to as the back-surface temperature.

Some specimens which were tested at the more severe stream conditions were modified by the addition of an asbestos phenolic shroud which is also shown in figure 1. The shrouded specimens had a 3.15-in-diameter (80 mm) flat face and a 20° flared afterbody.

Specimens were mounted in a water-cooled sting which protected the back-surface sensor from heating in all directions except through the test material.

TEST CONDITIONS AND PROCEDURE

The 2500-kilowatt arc jet at the Langley Research Center was used for this investigation. Descriptions of this facility are given in references 9 to 11. Nominal values of test stream conditions are given in table II. Each condition is identified by a letter from A to G and a symbol which is used in the text and in the figures, respectively. For convenience, conditions A, B, and C are referred to as moderate test conditions, D and E as severe conditions, and F and G as intermediate test conditions. Specimens of each material were tested at conditions A to E. Two of the materials were also tested at intermediate conditions F and G.

The test stream enthalpy and dynamic pressure were obtained by adjusting the electrical power input to the arc and the stream mass flow rate. These conditions and also the ablation specimen stagnation-point heat-transfer rates were determined from calibration tests.

Test Stream Composition

The test stream was a mixture of air and nitrogen with the flow rate of each gas regulated to provide a stream composition of 3 percent oxygen and approximately 97 percent nitrogen. This modification of stream composition from that of air was made to reduce the oxidizing effect of the low enthalpy test stream to match the oxidizing effect of air at high enthalpy values associated with reentry. In reference 4 the relation between enthalpy and oxygen concentration in two different streams having the same oxidizing effect is

$$\frac{C_{e,1}}{C_{e,2}} = \frac{(h_e - h_w)_1}{(h_e - h_w)_2} \quad (1)$$

From the relation, the oxidizing effect of the present test stream is equivalent to that of air with a stagnation enthalpy approximately $6\frac{2}{3}$ times greater than that of the test stream.

Dynamic Pressure

The dynamic pressure is

$$q_{\infty} = \frac{\rho_{\infty} U_{\infty}^2}{2} = \frac{p_t - p_{\infty}}{F_c} \quad (2)$$

where the compressibility factor F_c is given in reference 11.

The pressure rise measured in the arc chamber was the difference between stream total pressure and atmospheric pressure:

$$p_c = p_t - p_A \quad (3)$$

However, if the static pressure was assumed to be atmospheric,

$$p_{\infty} = p_A \quad (4)$$

then the dynamic pressure was approximately

$$q_{\infty} = \frac{p_c}{F_c} \quad (5)$$

The value of F_c was substantially different from 1 only when the 2-in-diameter (50.8 mm) nozzle was used at high flow rates.

Enthalpy

Static enthalpy was determined from the arc-chamber pressure rise by the method presented in reference 11. Stagnation enthalpy was then obtained from the charts of reference 12 by assuming an isentropic compression from static conditions to stagnation conditions. For the test conditions at low pressure there was not a significant difference in the values of static and stagnation enthalpy. The difference in static and stagnation values was significant only for test conditions D and E.

Static enthalpy was obtained with the method of reference 11 for test conditions C to G. However, at test conditions A and B it was not possible to obtain an accurate measurement of arc-chamber pressure which is necessary in order to use this method. Consequently, static temperature measurements were obtained at test conditions A to E by the spectrometric method described in reference 13. Static enthalpy was then obtained for a pressure of $p_{\infty} = 1 \text{ atm}$ ($1 \text{ atm} = 0.1013 \text{ MN/m}^2$) from the charts of reference 12.

The enthalpy values obtained from spectrometric measurements are given in a separate column in table II. These values are slightly higher than the values obtained from the pressure-rise method of reference 11. A comparison of enthalpy values obtained by these two methods is also given in reference 11, and a similar result is noted.

Heat-Transfer Rate

Heat-transfer rate was measured on the surface of a calorimeter having shape and dimensions identical to the ablation specimens. Two calorimeter shapes were used, one corresponding to the cylindrical specimen shape and the other corresponding to the truncated conical shape.

The temperature-rise rate was measured on the back surface of a 0.030-in-thick (0.8 mm) inconel sheet which constituted the front surface of the calorimeter model. Cold-wall heat-transfer rate was calculated from the temperature-rise rate and the thermophysical properties of inconel by the formula

$$\dot{q} = (c_p \rho x) \frac{dT}{dt} \quad (6)$$

Test Procedure

The tests were performed in a manner similar to that described in references 3, 7, and 9. The arc jet was operated for several minutes to allow stream conditions to stabilize. The calorimeter was then positioned in the stream momentarily to obtain a heat-transfer-rate measurement. The material specimen was positioned in the test stream upon removal of the calorimeter, and temperature rise on the back-surface sensor was recorded. When a back-surface temperature rise at $\Delta T = 600^\circ \text{R}$ (333°K) was reached, the test was terminated. After the specimen was withdrawn from the stream, the back-surface temperature rise was recorded until a maximum value was reached and a decrease was noted. A second heat-transfer measurement was made immediately after removing the specimen from the stream.

Color motion pictures were taken of most tests. From these films it was possible to observe the reaction of the model during exposure. Also, still photographs were made of each specimen after testing. The specimens were then coated with a thin layer of clear epoxy and sectioned on the diameter. Measurements of char-layer thickness and undegraded layer thickness of each specimen were made on the sectioned surface. The sectioned surface was then photographed.

RESULTS

The results of all tests are summarized in table III. This information includes the test conditions identified by the letters used in table II and the heating rate measured in each test. Specimen dimensions include the mass per unit area and thickness before testing and the thickness of the degraded char layer and the layer of undegraded material after testing. The back-surface temperature history is described by the exposure times at which temperature-rise values of 50° R (28° K), 100° R (56° K), 300° R (167° K), and 600° R (333° K) were indicated at the back-surface sensor. Back-surface temperature history is further described by the time and temperature at termination of exposure and the maximum temperature rise and time at which it occurred after termination of exposure. In some tests the back-surface temperature rise did not reach 600° R (333° K), the nominal value for termination of exposure. Such tests were usually terminated early because of equipment malfunction. The maximum back-surface temperature rise is not given for most of the tests at severe conditions (conditions D and E). The temperature-rise rate at termination of exposure at these conditions was extremely high as a result of material being completely removed from the sensor.

Appearance of Exposed Materials

Photographs of each material before and after testing are shown in figures 2 to 7. Each part of the figures represents a particular material at one test condition and shows an oblique view of the surface before and after exposure, a complete view of the sectioned surface of the tested specimen, and an enlarged view of the sectioned surface. An outline of the original specimen shape is shown on the full section view so that shape changes as a result of exposure are evident. The enlarged cross-section view shows details of the residual material such as the characteristics of the char, the interface between the char layer and undegraded layer, when this existed, and the attachment of the residual material to the back-surface sensor and mounting ring.

Char Surface and Interface Positions

A cross-section diagram of the residual layers which may exist after degradation of a char-producing material is shown in figure 8. Coordinates which describe the position and thickness of these layers are also shown. These positions were measured on the sectioned specimens at the center line referenced to the original specimen diameter. The thickness of the undegraded material layer x_i and the thickness of the char layer x_c are given in table III for each test.

In figure 9 the distance from the original front surface of the specimen to the char layer surface x_a and the distance from the original front surface to the char layer

undegraded material interface x_p are plotted against the total cold-wall heat load experienced by the specimens. The total stagnation-point heat load is the product of the cold-wall heating rate and the exposure time:

$$Q = \dot{q}t_f \quad (7)$$

The zero of the distance scale in figure 9 represents the original front surface of the specimen. Values above the zero position represent swelling and values below this position represent recession.

DISCUSSION

Thermal Shielding Effectiveness

A convenient parameter for evaluating thermal shielding performance is the cold-wall heat input to a unit mass of material required to produce a given temperature rise at the back-surface sensor. This shielding effectiveness is evaluated from experimental data in the following manner:

$$E_{\Delta T} = \frac{\dot{q}t_{\Delta T}}{w} \quad (8)$$

Effectiveness has been calculated for back-surface temperature-rise values of $\Delta T = 300^\circ \text{R}$ (167°K) from information given in table III and is shown as a function of heat-transfer rate in figure 10.

Shielding effectiveness is actually a function of several stream conditions such as heat-transfer rate, dynamic pressure, and enthalpy. There is evidence that shielding effectiveness also varies with unit mass. (See ref. 7.) It was difficult to separate the effect of each of these conditions since, in most cases, they varied simultaneously. The performance of each material must therefore be evaluated for the combined effect of all these parameters at each test condition. Although effectiveness of the six materials is plotted against cold-wall heating rate in figure 10, the values for other stream parameters at each test condition may be obtained from table II. The data points in figure 10 are identified by the symbols given in table II. The unit mass of each specimen is given in table III.

Effectiveness of the elastomeric materials increased with increasing heat-transfer rate and dynamic pressure at the moderate test conditions (A, B, and C) where heat-transfer rate was less than $100 \text{ Btu/ft}^2\text{-sec}$ (1.14 MW/m^2) and dynamic pressure was less than 50 lbf/ft^2 (2.4 kN/m^2). As the severity of the test conditions increased, the unshrouded E-1 specimens at intermediate test conditions F and G showed a smooth

transition from increasing to decreasing effectiveness. (See fig. 10(a).) The data for material E-2, shown in figure 10(b), also show a smooth transition and correlate with data from reference 3 taken over a similar range of conditions. At condition E the shrouded E-2 specimens experienced a moderate decrease in performance which agrees with the continuous trend of the data from reference 3. The E-1 and E-3 specimens tested at conditions D and E were not modified with a shroud as were the other specimens tested at the severe conditions. Therefore, the very abrupt decrease in performance experienced by these materials at the severe test conditions (figs. 10(a) and 10(c)) should not be compared with the performance of other materials in this range.

Shielding effectiveness of the rigid materials increased with increasing values of stream parameters at the moderate test conditions. However, the rigid materials did not, in general, experience a decrease in performance at the severe test conditions. Instead, the trend of effectiveness values tended to level off and approach a constant value with increasing heating rate and dynamic pressure. Effectiveness values for material R-3 were not obtained at severe test condition E because of equipment malfunction; however, the trend of these data suggests that the effectiveness of R-3 also approached a constant value.

Values of the effectiveness parameter in figure 10 can be compared as follows. Elastomeric material E-1 produced the highest values at moderate test conditions. In this range of conditions material E-2 ranked second whereas materials R-1 and R-2 ranked third. In the severe range of test conditions materials R-1 and R-2 produced the highest values of the effectiveness parameter.

Shielding Performance and Condition of the Materials

In order to make a realistic evaluation of overall shielding performance, it is necessary to compare the results indicated by the effectiveness parameter in figure 10 with the condition of the materials after exposure as shown in the photographs of figures 2 to 7, and the recession of the char surface and interface shown in figure 9.

At the moderate test conditions (A, B, and C) the materials which produced acceptable performance showed a symmetrical variation of thickness across the specimen diameter. Materials which showed poor performance at the moderate test conditions experienced varying degrees of uneven ablation. However, at the severe test conditions (D and E) all the materials tended to experience uneven ablation as a result of the combination of higher heating rate and dynamic pressure which produced high shear force at the edge of the specimen.

The first materials tested at the severe condition were the elastomeric E-1 specimens shown in figures 2(d) and 2(e) and the E-3 specimens shown in figures 4(d) and 4(e).

In these photographs, it is shown that large quantities of material were removed from the edge of the specimen in an uneven manner. It was believed that a specimen configuration which would resist the eroding shear force at the edge of the specimen and allow the material to ablate near the center of the disk would give a more realistic evaluation of thermal shielding performance. A shroud machined from molded asbestos phenolic was bonded to the circumference of the specimens used in subsequent tests at these conditions. (See fig. 1.) Most of these specimens continued to experience some uneven removal of material near the edge and in a few cases the shroud was lost near the end of the test.

At the moderate test conditions, the elastomeric materials formed comparatively strong and symmetrical char layers. Char surface positions x_a were characterized by swelling and very slight recession while interface positions x_p showed moderate recession. (See figs. 9(a), 9(b), and 9(c).) The decrease in effectiveness of elastomeric materials in the severe range of conditions was accompanied by uneven removal of material over the specimen surface. In this range of conditions, char surface and interface recessions were higher and char layer thickness was smaller than for the moderate conditions.

Rigid material R-1, which produced intermediate values of effectiveness at moderate test conditions, also produced very strong char layers in this range of conditions although the char surface and interface recessions were somewhat greater than for elastomeric materials (fig. 9(d)). In the severe range of test conditions, material R-1 produced the highest values of effectiveness, but like the elastomeric materials, experienced uneven removal of material over the specimen surface. Char surface and interface recessions of material R-1 were somewhat irregular in the severe range of test conditions.

Rigid material R-2 produced effectiveness values comparable to those produced by material R-1 over the entire range of test conditions. However, the char produced by material R-2 was extremely fragile at all test conditions. The char surface and interface recession values at moderate test conditions were quite high (fig. 9(e)). At the severe test conditions, char surface and interface recessions were very high and were also irregular in that they did not follow a continuous trend with increasing heat load.

Rigid material R-3 produced comparatively low values of effectiveness over the entire range of test conditions. At moderate conditions the char layer was extremely fragile although char surface and interface recession formed a continuous trend with increasing heat load and the recession was moderate (fig. 9(f)). In the severe range of conditions the char actually appeared to be somewhat improved, probably as a result of the residual layer of unaffected material which supported the char.

The performance of all materials in the severe range of test conditions appeared to be marginal as a result of the uneven removal of material. This behavior may be at least partially attributed to the test configuration. The flat specimens mounted 90° to the test stream were designed to provide approximately one-dimensional heating for thermal performance evaluation. However, as explained previously, this arrangement resulted in shear force being concentrated at the edge of the specimen and the consequent uneven removal of material at this point. Further investigation with a configuration which provides a more even distribution of force over the specimen surface may show that these materials give satisfactory performance at conditions more severe than the range of the present tests where performance was satisfactory.

CONCLUDING REMARKS

The thermal shielding performance of three ablative materials with a silicone resin base and three ablative materials with an epoxy or phenolic resin base has been investigated at varying test stream conditions in an electric-arc-heated gas stream composed of approximately 97 percent nitrogen and 3 percent oxygen. Stagnation enthalpy varied from 1850 to 3370 Btu/lbm (4.3 to 7.8 MJ/kg), dynamic pressure varied from approximately 0 to 1000 lbf/ft² (48 kN/m²), and stagnation-point heat-transfer rate varied from 20 to 220 Btu/ft²-sec (0.23 to 2.5 MW/m²).

Silicone base materials produced the highest performance in a moderate range of conditions where the stagnation-point heat-transfer rate was less than 100 Btu/ft²-sec (1.14 MW/m²) and dynamic pressure was less than 50 lbf/ft² (2.4 kN/m²). A formulation designated as "LRC E1B2" produced the highest performance in this range.

In a more severe range of conditions where the stagnation-point heat-transfer rate was greater than 150 Btu/ft²-sec (1.7 MW/m²) and dynamic pressure was greater than 155 lbf/ft² (7.4 kN/m²), the performance of silicone materials deteriorated rapidly whereas the performance of phenolic and epoxy base materials continued to increase slightly. The material which produced the highest performance in this range of conditions was an epoxy silica composition in a phenolic-glass-fiber honeycomb matrix.

Langley Research Center,

National Aeronautics and Space Administration,

Langley Station, Hampton, Va., April 18, 1966,

124-08-03-10-23.

APPENDIX

CONVERSION OF U.S. CUSTOMARY UNITS TO SI UNITS

The International System of Units (SI) was adopted in October 1960 by the Eleventh General Conference on Weights and Measures held in Paris, France. Conversion factors required for units used herein are given in the following table:

Physical quantity	U.S. Customary Unit	Conversion factor (*)	SI Unit
Length	$\left\{ \begin{array}{l} \text{ft} \\ \text{in.} \end{array} \right.$	0.3048 0.0254	m m
Specific heat	Btu/lbm-°R	4.18×10^3	J/kg-°K
Enthalpy	Btu/lbm	2.32×10^3	J/kg
Mass-flow rate	lbm/ft ² -sec	4.88	kg/m ² -sec
Pressure or stress	lbf/ft ²	47.88	N/m ²
Heat load	Btu/ft ²	1.135×10^4	J/m ²
Heating rate	Btu/ft ² -sec	1.135×10^4	W/m ²
Temperature	°R = (°F + 459.67)	5/9	°K
Mass per unit area	lbm/ft ²	4.88	kg/m ²
Density	lbm/ft ³	16.02	kg/m ³

* Multiply value given in U.S. Customary Unit by conversion factor to obtain equivalent value in SI units.

Prefixes to indicate multiples of units are as follows:

Prefix	Multiple
mega (M)	10 ⁶
kilo (k)	10 ³
centi (c)	10 ⁻²
milli (m)	10 ⁻³

REFERENCES

1. Peters, Roger W.; and Wadlin, Kenneth L.: The Effect of Resin Composition and Fillers on the Performance of a Molded Charring Ablator. NASA TN D-2024, 1963.
2. Swann, Robert T.; Brewer, William D.; and Clark, Ronald K.: Effect of Composition and Density on the Ablative Performance of Phenolic-Nylon. Paper presented at VIII Natl. Meeting of Am. Soc. Aerospace Mater. Process Engr. (San Francisco), May 25-28, 1965.
3. Clark, Ronald K.: Effect of Environmental Parameters on the Performance of Low-Density Silicone-Resin and Phenolic-Nylon Ablation Materials. NASA TN D-2543, 1965.
4. Swann, Robert T.; Dow, Marvin B.; and Tompkins, Stephen S.: Analysis of the Effects of Environmental Conditions on the Performance of Charring Ablators. AIAA Entry Technology Conference, CP-9, Am. Inst. Aeron. Astronaut., Oct. 1964, pp. 259-269.
5. Dow, Marvin B.; and Swann, Robert T.: Determination of Effects of Oxidation on Performance of Charring Ablators. NASA TR R-196, 1964.
6. Swann, Robert T.: Approximate Analysis of the Performance of Char-Forming Ablators. NASA TR R-195, 1964.
7. Chapman, Andrew J.: Effect of Weight, Density, and Heat Load on Thermal-Shielding Performance of Phenolic Nylon. NASA TN D-2196, 1964.
8. Mechtly, E. A.: The International System of Units - Physical Constants and Conversion Factors. NASA SP-7012, 1964.
9. Chapman, Andrew J.: An Experimental Evaluation of Three Types of Thermal Protection Materials at Moderate Heating Rates and High Total Heat Loads. NASA TN D-1814, 1963.
10. Scott, Samuel J.: Subsonic Aerodynamic Heat Transfer to a Surface Recessed Within a Forward Stagnation Region Slit. NASA TN D-2034, 1963.
11. Brown, Ronald D.; and Fowler, Bruce: Enthalpy Calculated From Pressure and Flow-Rate Measurements in High-Temperature Subsonic Streams. NASA TN D-3013, 1965.
12. Fowler, Bruce; and Brown, Ronald D.: Charts for Approximate Thermodynamic Properties of Nitrogen-Oxygen Mixtures. NASA SP-3017, 1965.
13. Greenshields, David H.: Spectrometric Measurements of Gas Temperatures in Arc-Heated Jets and Tunnels. NASA TN D-1960, 1963.

TABLE I.- TEST MATERIALS

[All materials were reinforced by a phenolic-glass-fiber honeycomb matrix which had $\frac{3}{16}$ to $\frac{1}{4}$ in. (4.76 to 6.35 mm) hexagonal cells and a density of 4 to 9 lbm/ft³ (64 to 144 kg/m³)

Material	Source	Name	Composition	Specific gravity
E-1	Langley Research Center	E1B2	Silicone resin 75% mass (Sylgard 182) Silica microspheres 15% mass (Eccospheres SI) Microballoons 10% mass (Made of BJO-0930 phenolic resin)	0.67
E-2	Dow Corning	325	Silicone resin with additives	0.93
E-3	General Electric Company	ESM 1000	Foamed silicone resin with additives	0.79
R-1	AVCO Corporation	Avcoat 5026-39	Epoxy resin Silica Phenolic Microballoons	0.61
R-2	Ling-Temco-Vought, Inc.	Melamine phenolic	Melamine resin Phenolic resin Phenolic microballoons Chopped quartz	0.71
R-3	Emerson Electric Manufacturing Company	Thermolag T-500	Inorganic salts Phenolic resin	1.38

TABLE II.- NOMINAL TEST CONDITIONS

Test condition	Power, kW	Stream diameter		Mass-flow rate per unit area, m/A		Dynamic pressure, q _∞		Enthalpy								Stagnation-point heat-transfer rate, q̇	
								Pressure-rise method				Spectrographic method					
		h _∞	h _s		h _∞		h _s										
in.	cm	$\frac{\text{lbm}}{\text{ft}^2\text{-sec}}$	$\frac{\text{kg}}{\text{m}^2\text{-s}}$	$\frac{\text{lbf}}{\text{ft}^2}$	$\frac{\text{kN}}{\text{m}^2}$	$\frac{\text{Btu}}{\text{lbm}}$	$\frac{\text{MJ}}{\text{kg}}$	$\frac{\text{Btu}}{\text{lbm}}$	$\frac{\text{MJ}}{\text{kg}}$	$\frac{\text{Btu}}{\text{lbm}}$	$\frac{\text{MJ}}{\text{kg}}$	$\frac{\text{Btu}}{\text{lbm}}$	$\frac{\text{MJ}}{\text{kg}}$	$\frac{\text{Btu}}{\text{ft}^2\text{-sec}}$	$\frac{\text{MW}}{\text{m}^2}$		
Moderate																	
A ○	1100	12	30.48	0.19	0.92	----	----	----	----	2300	5.34	2300	5.34	22	0.25		
B □	1200	6	15.24	.77	3.73	----	----	----	----	2300	5.34	2300	5.34	48	.54		
C ◇	1650	4	10.16	4.02	19.50	47	2.25	2300	5.34	2300	5.34	2600	6.03	2600	6.03	88	1.00
Severe																	
D ▲	1750	2	5.08	16.05	77.80	800	38.30	2450	5.68	2500	5.80	2950	6.84	3030	7.03	150	1.70
E ▽	2300	2	5.08	16.05	77.80	1000	47.88	3200	7.42	3370	7.82	3700	8.59	3850	8.94	220	2.50
Intermediate																	
F ◇	1025	2	5.08	6.88	33.40	115	5.50	1850	4.29	1850	4.29	----	---	----	---	100	1.13
G ▢	1700	2	5.08	6.88	33.40	155	7.42	2650	6.15	2700	6.26	----	---	----	---	155	1.76

TABLE III.- TEST RESULTS

(a) Material E-1

Test condition	Heat-transfer rate, \dot{q}		Specimen dimensions								Back-surface temperature											
			Before test				After test				Exposure time, $t_{\Delta T}$, sec, for -				Termination of exposure			Maximum temperature rise				
			Mass per unit area, w		Thickness, x_o		Char layer thickness, x_c		Undegraded layer thickness, x_i													
			Btu ft ² -sec	MW m ²	lbm ft ²	kg m ²	in.	cm	in.	cm											in.	cm
	$\Delta T = 50^{\circ}\text{R}$ (28° K)	$\Delta T = 100^{\circ}\text{R}$ (56° K)	$\Delta T = 300^{\circ}\text{R}$ (167° K)	$\Delta T = 600^{\circ}\text{R}$ (333° K)	t_f sec	ΔT_f °R	°K	t_m sec	ΔT_m °R	°K												
A	23	0.26	1.06	5.17	0.31	0.79	0.35	0.89	0	0	68	97	220	338	342	615	342	391	693	385		
A	21	.24	1.06	5.17	.31	.79	.34	.86	0	0	67	---	226	315	322	614	341	347	646	359		
B	49	.56	2.14	10.44	.54	1.37	.65	1.65	0	0	125	183	336	425	429	614	341	494	717	398		
B	50	.57	2.14	10.44	.54	1.37	.64	1.63	0	0	115	190	317	422	429	621	345	482	717	398		
B	53	.60	3.00	14.64	.86	2.18	.47	1.19	.42	1.07	144	---	---	---	210	95	53	430	177	98		
C	94	1.07	3.18	15.52	.92	2.34	.87	2.21	0	0	82	165	357	448	459	650	361	540	934	519		
C	93	1.06	3.19	15.57	.92	2.34	.88	2.24	0	0	163	273	438	530	534	612	340	607	670	372		
C	83	.94	3.00	14.64	.87	2.21	.81	2.06	0	0	176	250	403	511	520	632	351	597	780	433		
D	177	2.01	4.26	20.79	1.23	3.12	.15	.38	.52	1.32	152	---	153	154	155	771	428	---	---	---		
D	170	1.93	4.26	20.79	1.23	3.12	.24	.61	.74	1.88	---	---	---	---	112	101	56	---	---	---		
E	252	2.86	6.32	30.84	1.82	4.62	.02	.05	1.00	2.54	83	---	85.5	86	91	---	---	---	---	---		
E	197	2.24	6.32	30.84	1.82	4.62	.06	.15	.70	1.78	149.6	---	150	150.5	151	---	---	---	---	---		
E	196	2.22	3.00	14.64	.87	2.21	.15	.38	.20	.51	---	---	---	---	121	0	0	---	63	35		
E	229	2.60	3.00	14.64	.87	2.21	.14	.36	.42	.42	---	---	---	---	71	0	0	---	15	8		
F	100	1.14	3.00	14.64	.87	2.21	.80	2.03	0	0	297	354	444	530	539	632	351	641	794	441		
F	98	1.11	3.00	14.64	.88	2.23	.81	2.06	0	0	315	366	451	530	531	609	338	695	810	450		
G	155	1.76	3.00	14.64	.87	2.21	.14	.36	0	0	199	212	232	248	253	852	473	264	968	538		
G	161	1.83	3.00	14.64	.88	2.23	.14	.36	0	0	220	215	234.5	250	251	825	347	267	738	410		
G	155	1.76	3.00	14.64	.87	2.21	.16	.41	0	0	198	211	231	---	235	354	197	270	510	283		

(b) Material E-2

Test condition	Heat-transfer rate, \dot{q}		Specimen dimensions								Back-surface temperature											
			Before test				After test				Exposure time, $t_{\Delta T}$, sec, for -				Termination of exposure			Maximum temperature rise				
			Mass per unit area, w		Thickness, x_o		Char layer thickness, x_c		Undegraded layer thickness, x_i													
			Btu ft ² -sec	MW m ²	lbm ft ²	kg m ²	in.	cm	in.	cm											in.	cm
											$\Delta T = 50^{\circ}\text{R}$ (28 ^o K)	$\Delta T = 100^{\circ}\text{R}$ (56 ^o K)	$\Delta T = 300^{\circ}\text{R}$ (167 ^o K)	$\Delta T = 600^{\circ}\text{R}$ (333 ^o K)	t_f sec	ΔT_f °R °K	t_m sec	ΔT_m °R °K				
A	21	0.24	1.00	4.88	0.21	0.53	0.24	0.61	0.04	0.10	37	51	119	220	223	615 342	257	676 375				
A	21	.24	1.00	4.88	.21	.53	.24	.61	.04	.10	40	55	124	243	250	621 345	288	670 372				
B	47	.53	2.00	9.76	.42	1.07	.47	1.19	.06	.15	102	133	245	372	374	609 338	429	696 387				
B	48	.55	2.00	9.76	.42	1.07	.46	1.17	.04	.10	104	137	237	350	361	644 358	419	737 409				
C	93	1.06	3.00	14.64	.63	1.60	.67	1.70	0	0	140	192	316	410	416	635 353	482	847 471				
C	93	1.06	3.00	14.64	.63	1.60	.65	1.65	0	0	141	196	323	406	426	705 392	481	870 483				
D	147	1.67	4.00	19.52	.84	2.13	.17	.43	.24	.61	201	203	205	---	206	1380 767	---	---	---			
G	151	1.71	4.00	19.52	.83	2.10	.24	.61	0	0	205	231	279	306	308	1390 772	---	---	---			
E	218	2.48	6.01	29.33	1.25	3.18	.10	.25	.12	.30	266	274	277	278	278.3	684 380	---	---	---			
E	207	2.35	6.01	29.33	1.25	3.18	.12	.30	.04	.10	252	267	274	275	275	600 333	---	---	---			

TABLE III.- TEST RESULTS - Continued

(c) Material E-3

Test condition	Specimen dimensions										Back-surface temperature									
	Heat-transfer rate, \dot{q}		Before test				After test				Exposure time, $t_{\Delta T}$, sec, for -				Termination of exposure			Maximum temperature rise		
			Mass per unit area, w		Thickness, x_o		Char layer thickness, x_c		Undegraded layer thickness, x_i											
															t_f	ΔT_f		t_m	ΔT_m	
	$\frac{\text{Btu}}{\text{ft}^2\text{-sec}}$	$\frac{\text{MW}}{\text{m}^2}$	$\frac{\text{lbm}}{\text{ft}^2}$	$\frac{\text{kg}}{\text{m}^2}$	in.	cm	in.	cm	in.	cm	$\Delta T = 50^{\circ}\text{R}$ (28 $^{\circ}\text{K}$)	$\Delta T = 100^{\circ}\text{R}$ (56 $^{\circ}\text{K}$)	$\Delta T = 300^{\circ}\text{R}$ (167 $^{\circ}\text{K}$)	$\Delta T = 600^{\circ}\text{R}$ (333 $^{\circ}\text{K}$)	sec	$^{\circ}\text{R}$	$^{\circ}\text{K}$	sec	$^{\circ}\text{R}$	$^{\circ}\text{K}$
	A	21	0.24	1.06	5.17	0.26	0.66	0.24	0.61	0.08	0.20	42	58	118	224	230	614	341	278	693
A	22	.25	1.06	5.17	.26	.66	.23	.58	.10	.25	43	59	124	263	266	606	337	311	684	380
B	40	.46	2.11	10.30	.52	1.32	.53	1.35	.06	.15	104	139	223	318	326	617	343	396	760	422
B	39	.44	2.11	10.30	.52	1.32	.48	1.22	.07	.18	80	127	229	327	330	612	340	389	742	412
C	91	1.03	3.14	15.30	.77	1.96	.73	1.85	0	0	119	171	272	364	370	624	347	470	879	488
C	89	1.01	3.14	15.30	.77	1.96	.73	1.85	0	0	65	131	257	347	357	629	349	450	922	512
D	177	2.01	4.12	20.10	1.01	2.57	---	---	.28	.71	---	---	---	99	100	---	---	---	---	---
D	177	2.01	4.17	20.35	1.02	2.59	---	---	.33	.84	---	---	---	107	108	---	---	---	---	---
E	255	2.90	6.34	30.94	---	---	---	---	---	---	74	---	---	75	86	---	---	---	---	---
E	254	2.89	6.26	30.55	1.54	3.91	.06	.15	.38	.97	82	---	---	83	84	---	---	---	---	---

(d) Material R-1

Test condition	Specimen dimensions										Back-surface temperature									
	Heat-transfer rate, \dot{q}		Before test				After test				Exposure time, $t_{\Delta T}$, sec, for -				Termination of exposure		Maximum temperature rise			
			Mass per unit area, w		Thickness, x_o		Char layer thickness, x_c		Undegraded layer thickness, x_i											
	t_f	ΔT_f	t_m	ΔT_m																
Btu ft ² -sec	MW m ²	lbm ft ²	kg m ²	in.	cm	in.	cm	in.	cm	$\Delta T = 50^{\circ}\text{ R}$ (28 $^{\circ}\text{ K}$)	$\Delta T = 100^{\circ}\text{ R}$ (56 $^{\circ}\text{ K}$)	$\Delta T = 300^{\circ}\text{ R}$ (167 $^{\circ}\text{ K}$)	$\Delta T = 600^{\circ}\text{ R}$ (333 $^{\circ}\text{ K}$)	sec	$^{\circ}\text{R}$	$^{\circ}\text{K}$	sec	$^{\circ}\text{R}$	$^{\circ}\text{K}$	
A	23	0.26	1.00	4.88	0.29	0.74	0.31	0.79	0	0	50	67	122	203	211	632	351	244	714	397
A	23	.26	1.00	4.88	.28	.71	.31	.79	0	0	52	70	128	213	220	635	353	258	731	406
B	51	.58	2.14	10.44	.64	1.63	.61	1.55	0	0	100	146	249	323	326	626	348	386	870	483
B	53	.60	2.14	10.44	.67	1.70	.61	1.55	0	0	113	154	255	324	330	632	351	395	919	511
C	86	.98	3.21	15.66	.97	2.46	.70	1.78	0	0	138	205	340	407	410	638	354	465	1061	589
C	86	.98	3.21	15.66	.98	2.49	.68	1.73	0	0	105	176	328	393	396	638	354	443	1024	569
C	80	.91	2.98	14.55	.95	2.41	.75	1.90	0	0	104	154	301	375	377	624	347	457	908	504
D	132	1.50	4.28	20.90	1.37	3.48	.20	.51	.28	.71	270	271	273	274	274	600	333	---	---	---
D	171	1.94	4.28	20.90	1.36	3.46	.20	.51	.18	.46	250	264	274	275	276	766	425	---	---	---
E	231	2.62	6.42	31.33	1.99	5.06	.25	.64	.02	.05	324	332	336	337	337	600	333	---	---	---
E	226	2.56	6.42	31.33	1.97	5.00	.24	.61	.12	.30	342	---	---	---	347	79	44	433	362	201
E	219	2.49	3.00	14.64	.93	2.36	---	---	---	---	156	158	---	159	160	---	---	---	---	---

TABLE III.- TEST RESULTS - Concluded

(e) Material R-2

Test condition	Heat-transfer rate, \dot{q}		Specimen dimensions								Back-surface temperature											
			Before test				After test				Exposure time, $t_{\Delta T}$, sec, for -				Termination of exposure			Maximum temperature rise				
			Mass per unit area, w		Thickness, x_o		Char layer thickness, x_c		Undegraded layer thickness, x_i													
	Btu ft ² -sec	MW m ²	lbm ft ²	kg m ²	in.	cm	in.	cm	in.	cm	$\Delta T = 50^{\circ}\text{R}$ (28° K)	$\Delta T = 100^{\circ}\text{R}$ (56° K)	$\Delta T = 300^{\circ}\text{R}$ (167° K)	$\Delta T = 600^{\circ}\text{R}$ (333° K)	t_f sec	ΔT_f °R °K	t_m sec	ΔT_m °R °K				
A	23	0.26	1.01	4.93	0.21	0.53	0.24	0.61	0	0	44	62	135	210	218	638 354	245	702 390				
A	24	.27	1.01	4.93	.24	.61	.24	.61	0	0	46	62	131	209	214	626 348	245	685 381				
B	48	.55	2.01	9.81	.48	1.22	.46	1.17	0	0	100	135	233	259	263	638 354	265	644 358				
B	47	.53	2.00	9.76	.49	1.24	.42	1.07	0	0	98	138	265	350	353	632 351	405	905 503				
C	83	.94	2.66	12.98	1.08	2.74	.70	1.78	0	0	108	165	295	329	331	640 356	375	1076 598				
C	82	.93	2.65	12.93	1.08	2.74	.62	1.57	0	0	94	160	250	282	283	615 342	346	934 519				
D	153	1.74	3.85	18.79	1.36	3.46	.32	.81	0	0	279	---	280	281	282	1143 634	---	----				
D	120	1.36	3.84	18.74	1.36	3.46	.27	.69	0	0	---	275	282	---	283	1014 563	---	----				
E	240	2.73	5.69	27.77	1.97	5.00	.13	.33	0	0	271	274	---	275	275	600 333	---	----				
E	211	2.40	5.95	29.04	1.96	4.98	.17	.43	0	0	320	328	332	333	333	600 333	---	----				

(f) Material R-3

Test condition	Heat-transfer rate, \dot{q}		Specimen dimensions								Back-surface temperature											
			Before test				After test				Exposure time, $t_{\Delta T}$, sec, for -				Termination of exposure		Maximum temperature rise					
	Btu ft ² -sec	MW m ²	lbm ft ²	kg m ²	in.	cm	in.	cm	in.	cm	$\Delta T = 50^{\circ}\text{R}$ (28 ^o K)	$\Delta T = 100^{\circ}\text{R}$ (56 ^o K)	$\Delta T = 300^{\circ}\text{R}$ (167 ^o K)	$\Delta T = 600^{\circ}\text{R}$ (333 ^o K)	t_f sec	ΔT_f °R °K	t_m sec	ΔT_m °R °K				
A	23	0.26	1.00	4.88	0.14	0.36	0.18	0.46	0	0	21	31	88	185	191	635	353	218	757	420		
A	23	.26	1.00	4.88	.14	.36	.18	.46	0	0	21	33	99	183	188	638	354	211	731	406		
B	51	.58	2.14	10.44	.30	.76	.33	.84	0	0	64	90	186	279	282	610	339	318	808	449		
B	52	.59	2.14	10.44	.30	.76	.33	.84	0	0	65	88	206	262	265	655	364	298	864	480		
C	85	.97	3.21	15.66	.45	1.14	.39	.99	0	0	102	135	245	280	281	606	337	356	1038	577		
C	90	1.02	3.21	15.66	.45	1.14	.42	1.07	0	0	73	117	257	311	311	600	333	348	1122	623		
D	153	1.74	4.28	20.89	.59	1.50	.31	.79	.08	.20	154	190	255	257	257	600	333	---	----	---		
D	154	1.75	4.28	20.89	.60	1.52	.34	.86	0	0	160	199	290	294	294	600	333	---	----	---		
E	219	2.49	6.42	31.32	.89	2.26	.17	.43	.35	.89	---	---	---	---	218	26	14	444	137	76		
E	230	2.61	6.42	31.32	.89	2.26	.26	.66	.32	.81	---	---	---	---	226	47	26	430	152	84		

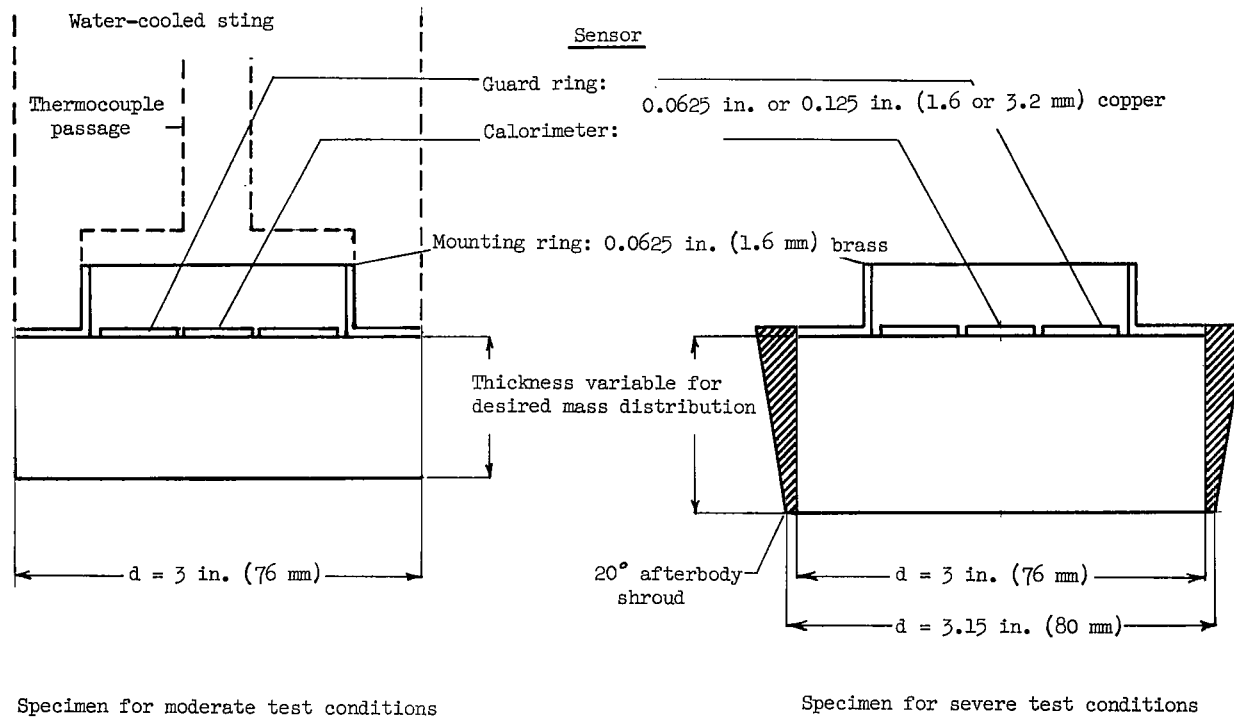
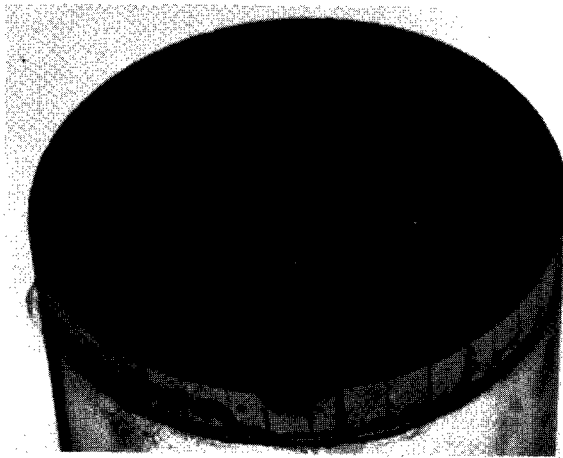
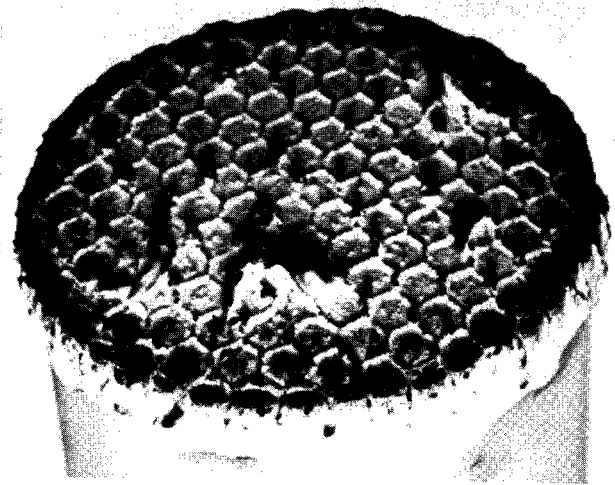


Figure 1.- Cross-section diagram of material specimen assemblies.



Front surface before test



Front surface after test



1 in.
1 cm

Sectioned specimen after test



0.5 in.
1 cm

Sectioned specimen after test (enlarged view)

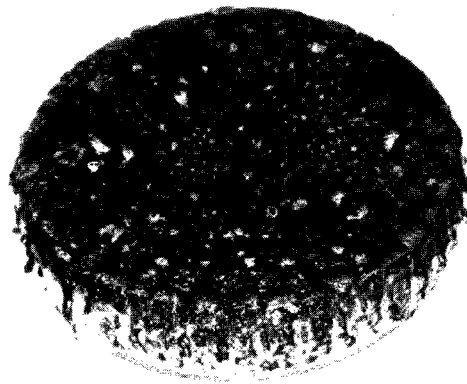
(a) Test condition A.

L-66-1141

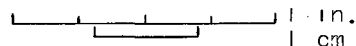
Figure 2.- Material E-1.



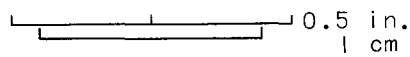
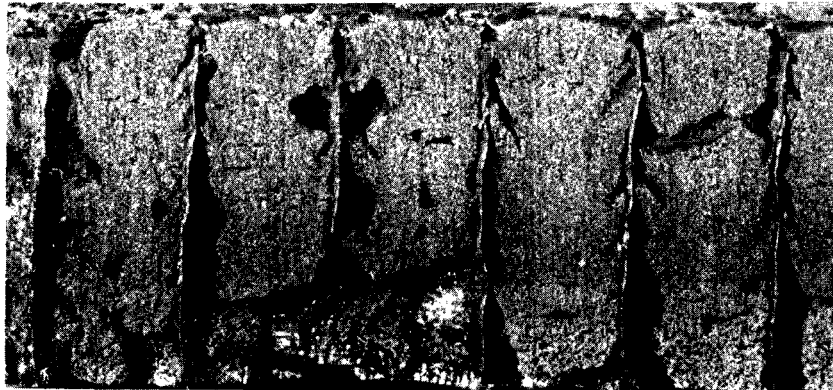
Front surface before test



Front surface after test



Sectioned specimen after test

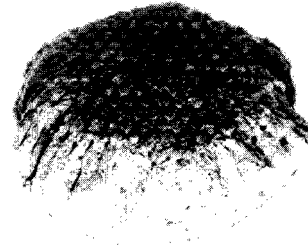
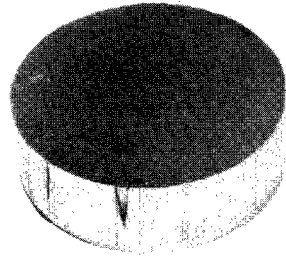


Sectioned specimen after test (enlarged view)

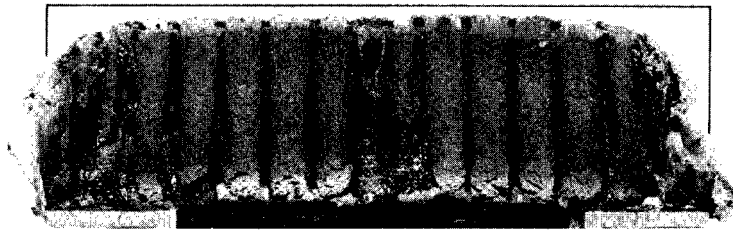
(b) Test condition B.

L-66-1142

Figure 2.- Continued.

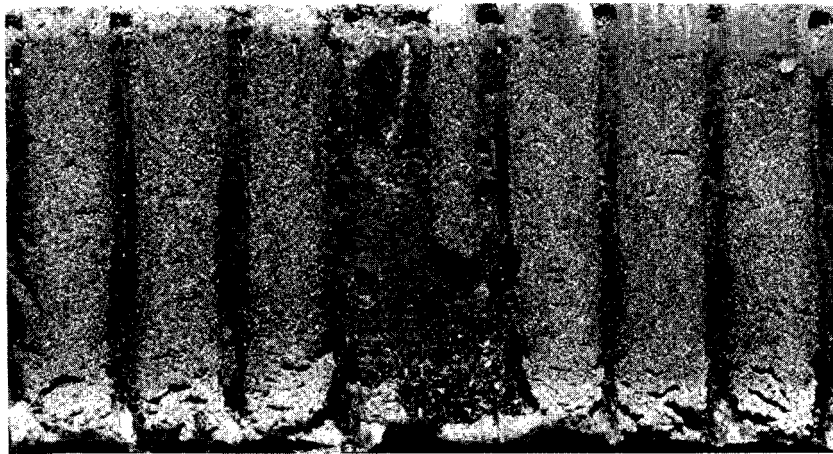


Front surface before test Front surface after test



1 in.
1 cm

Sectioned specimen after test



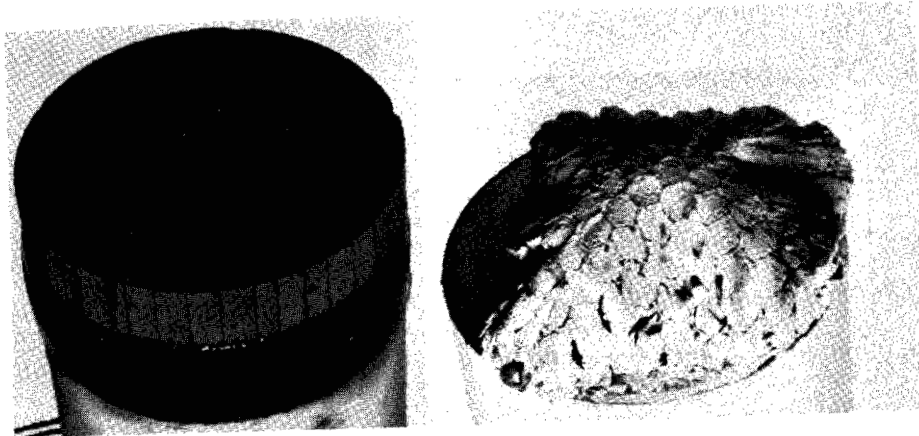
0.5 in.
1 cm

Sectioned specimen after test (enlarged view)

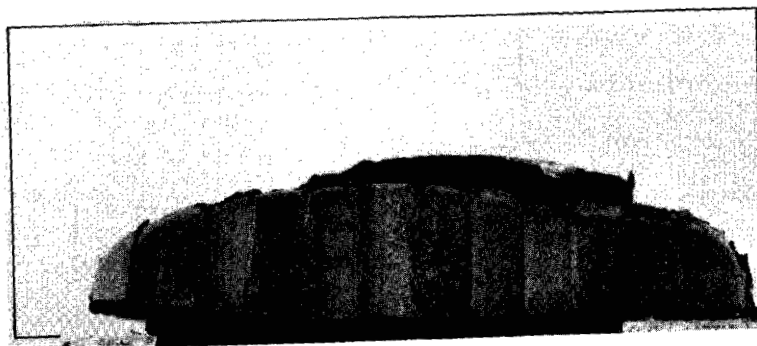
(c) Test condition C.

L-66-1143

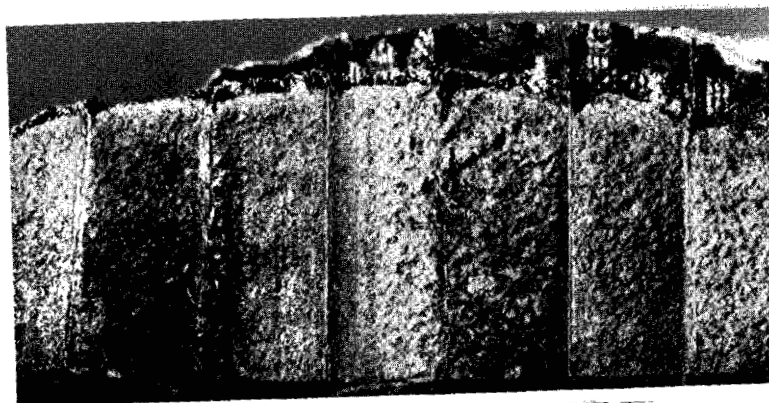
Figure 2.- Continued.



Front surface before test Front surface after test



Sectioned specimen after test

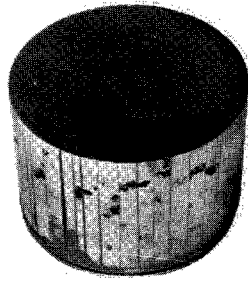


Sectioned specimen after test (enlarged view)

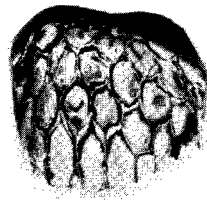
(d) Test condition D.

L-66-1144

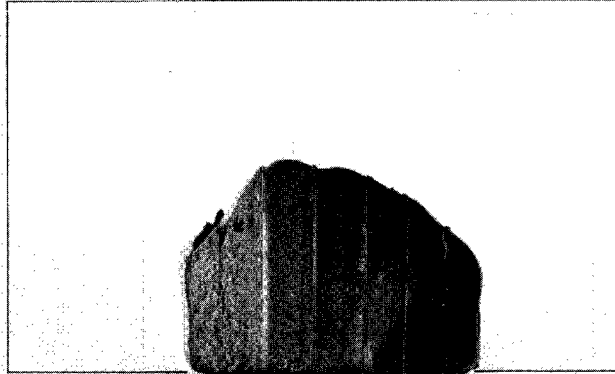
Figure 2,- Continued.



Front surface before test



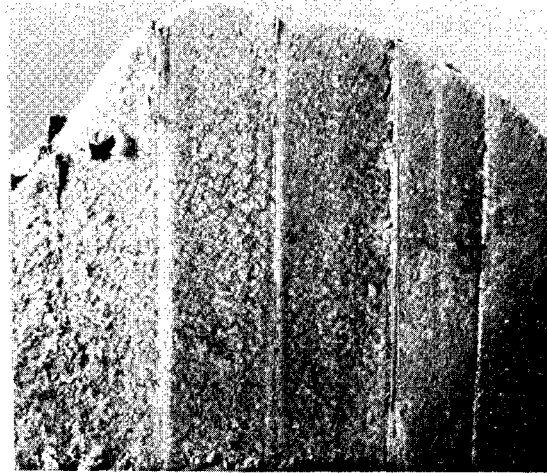
Front surface after test



1 in.

1 cm

Sectioned specimen after test



0.5 in.

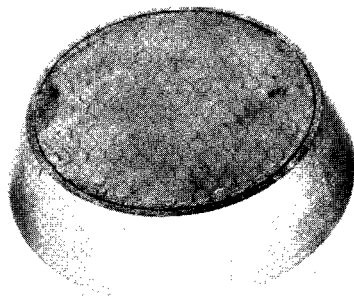
1 cm

Sectioned specimen after test (enlarged view)

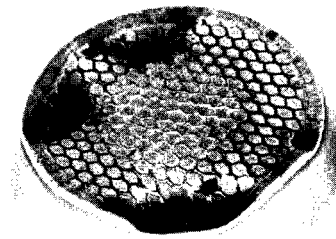
(e) Test condition E.

L-66-1145

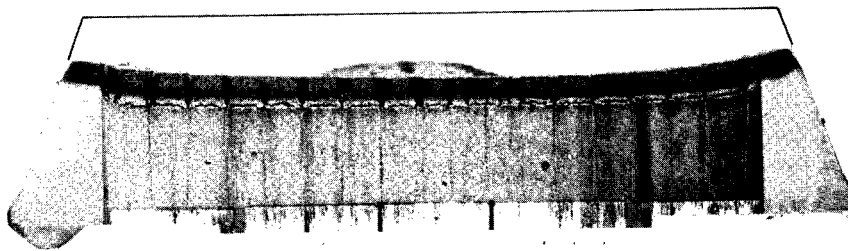
Figure 2.- Continued.



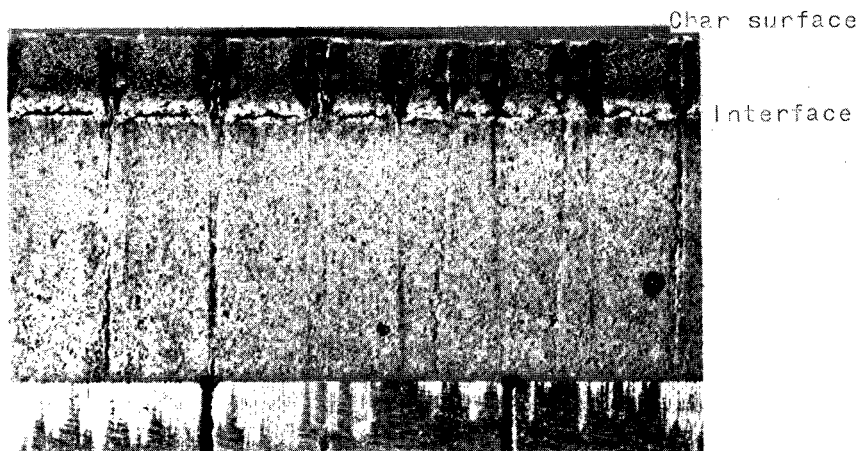
Front surface before test



Front surface after test



Sectioned specimen after test

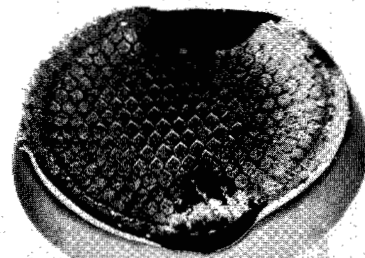
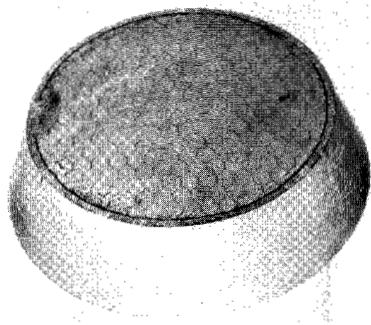


Sectioned specimen after test (enlarged view)

(f) Test condition E. Exposure time, 71 sec.

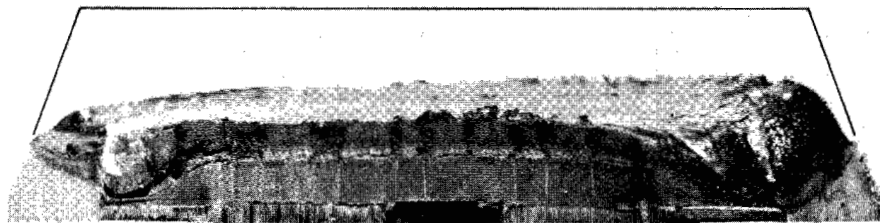
L-66-1146

Figure 2.- Continued.



Front surface before test

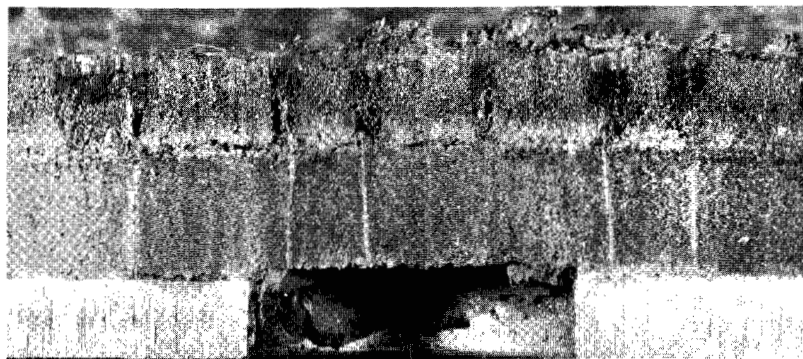
Front surface after test



1 in.

1 cm

Sectioned specimen after test



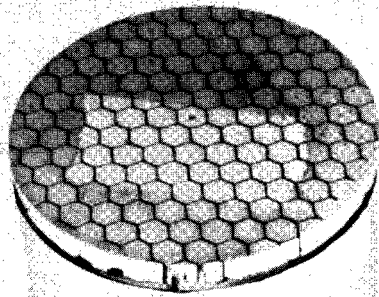
0.5 in.
1 cm

Sectioned specimen after test (enlarged view)

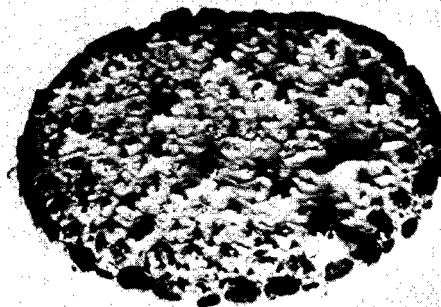
(g) Test condition E. Exposure time, 121 sec.

L-66-1147

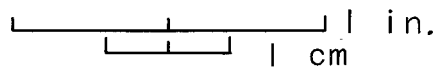
Figure 2.- Concluded.



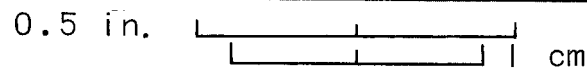
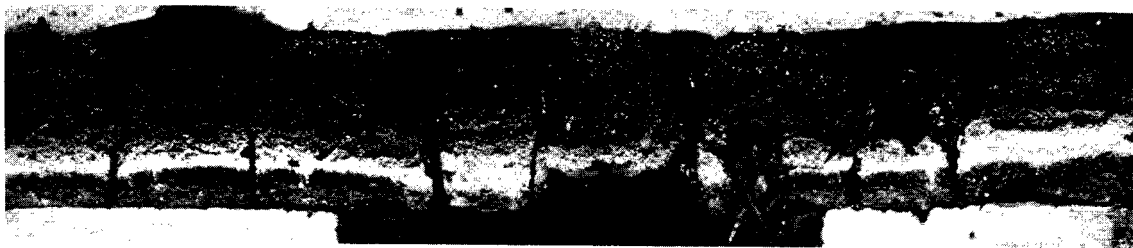
Front surface
before test



Front surface
after test



Sectioned specimen after test

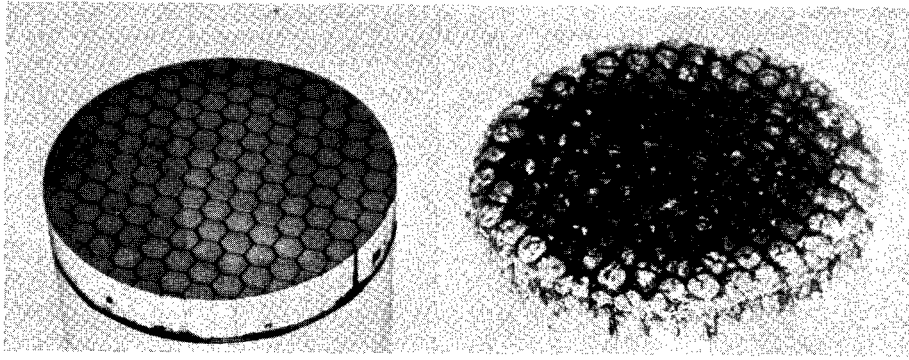


Sectioned specimen after test (enlarged view)

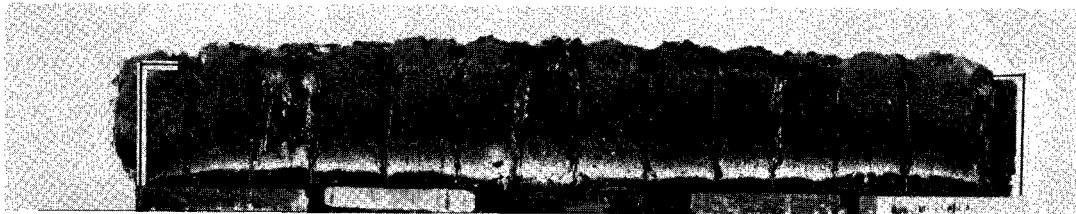
(a) Test condition A.

L-66-1148

Figure 3.- Material E-2.

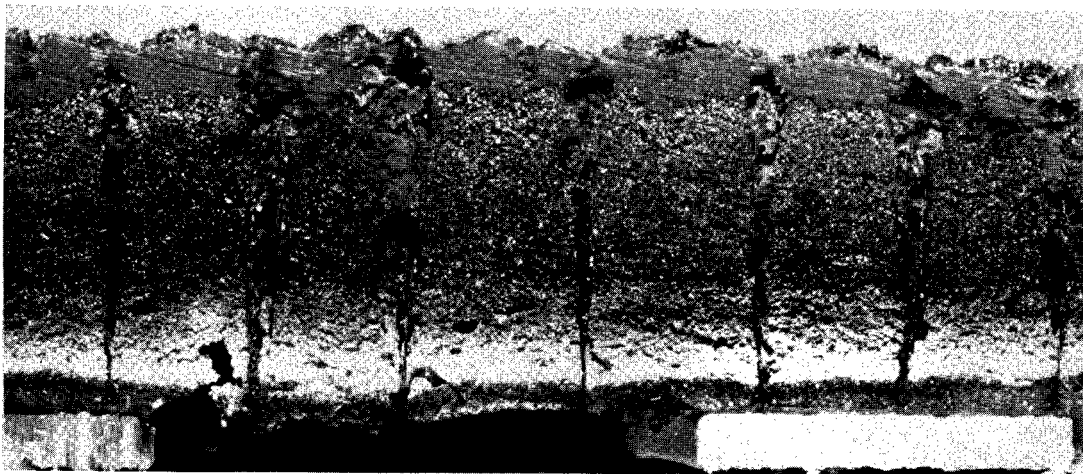


Front surface before test Front surface after test



1 in.
1 cm

Sectioned specimen after test



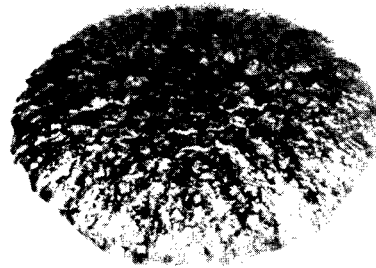
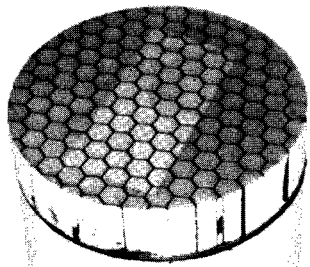
0.5 in.
1 cm

Sectioned specimen after test (enlarged view)

(b) Test condition B.

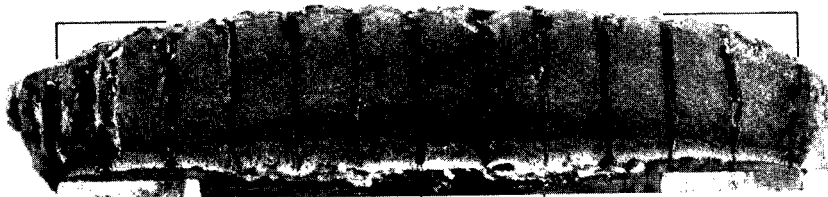
L-66-1149

Figure 3.- Continued.



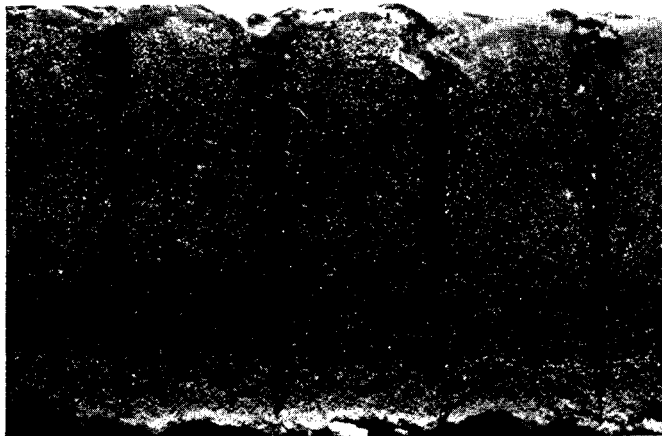
Front surface before test

Front surface after test



1 in.
1 cm

Sectioned specimen after test



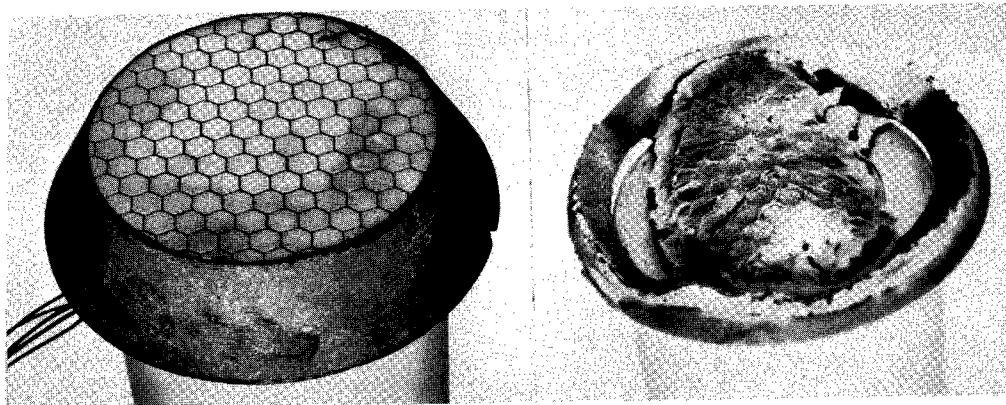
0.5 in.
1 cm

Sectioned specimen after test (enlarged view)

(c) Test condition C.

L-66-1150

Figure 3.- Continued.

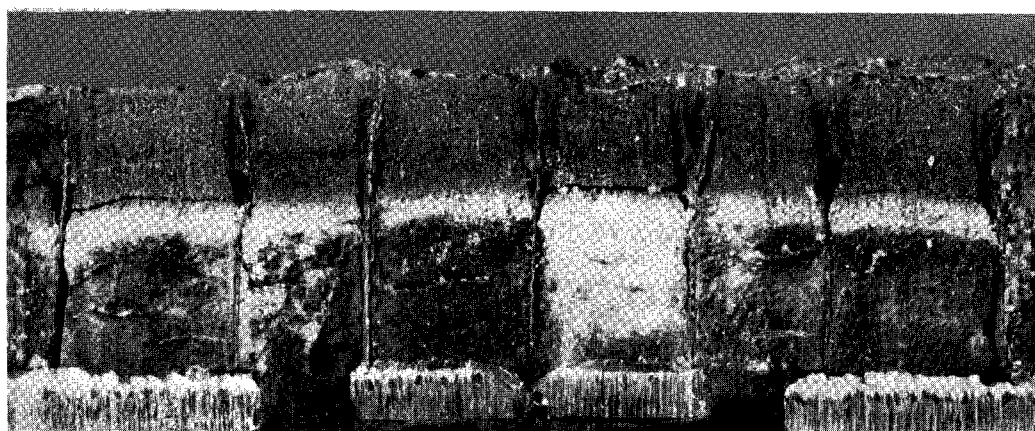


Front surface before test Front surface after test



1 in.
cm

Sectioned specimen after test



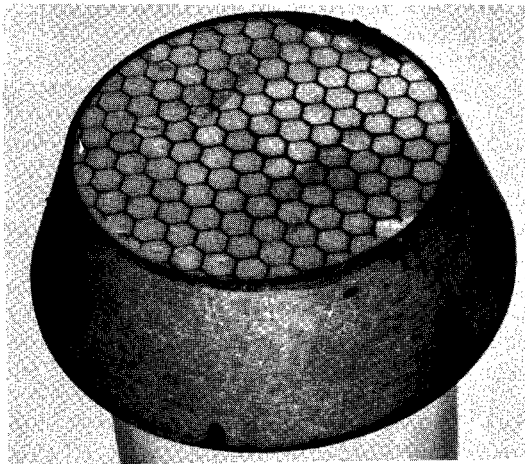
0.5 in.
cm

Sectioned specimen after test (enlarged view)

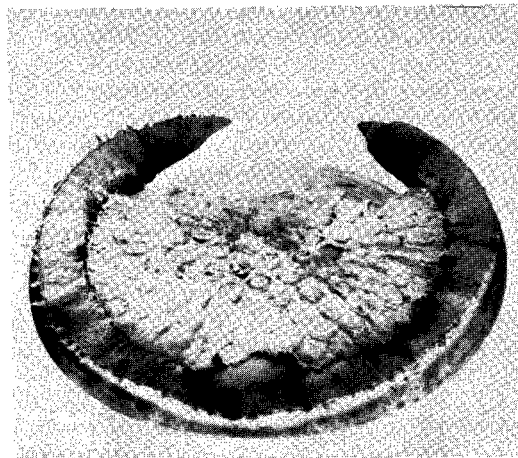
(d) Test condition D.

L-66-1151

Figure 3,- Continued.



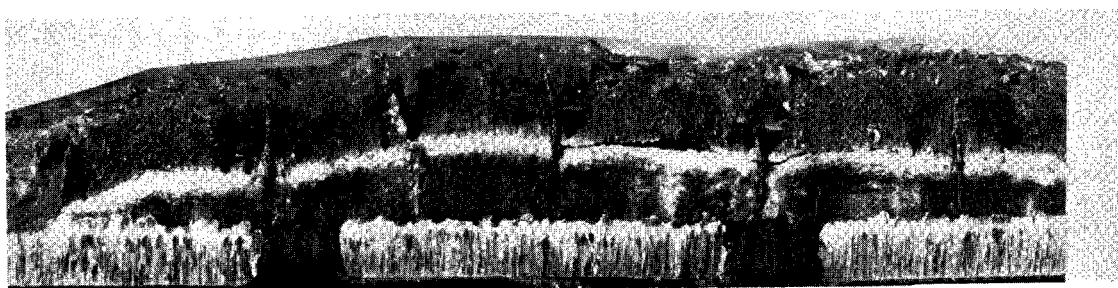
Front surface
before test



Front surface
after test



1 in.
1 cm
Sectioned specimen after test

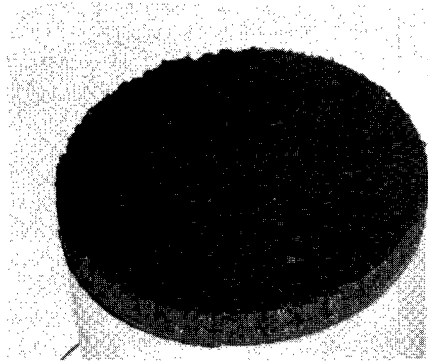


0.5 in.
1 cm
Sectioned specimen after test (enlarged view)

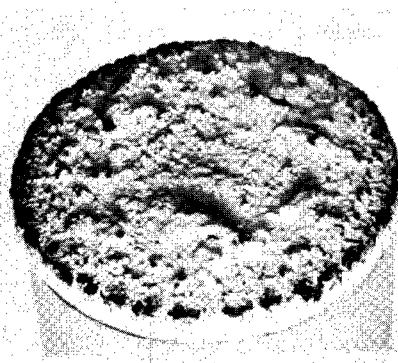
(e) Test condition E.

L-66-1152

Figure 3.- Concluded.



Front surface
before test

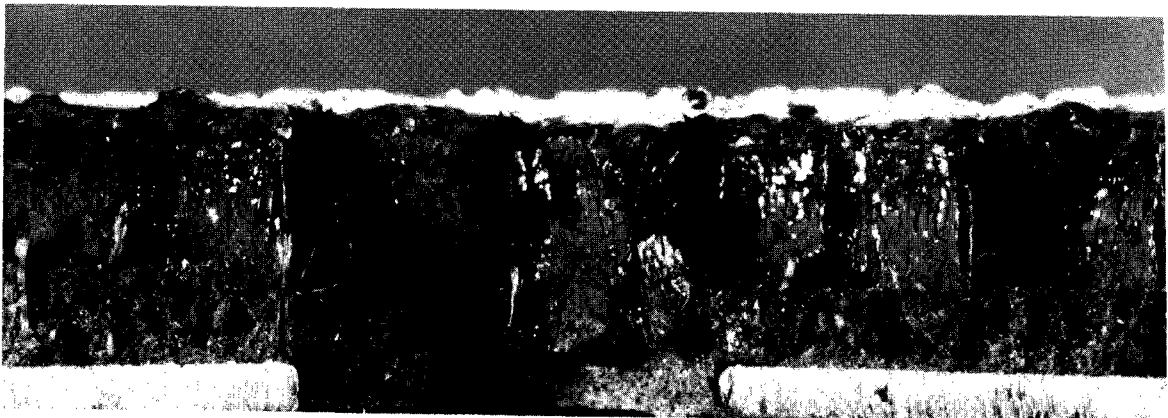


Front surface
after test



1 in.
1 cm

Sectioned specimen after test



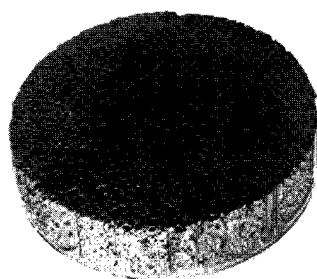
0.5 in.
1 cm

Sectioned specimen after test (enlarged view)

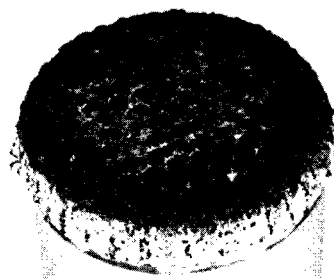
(a) Test condition A.

L-66-1153

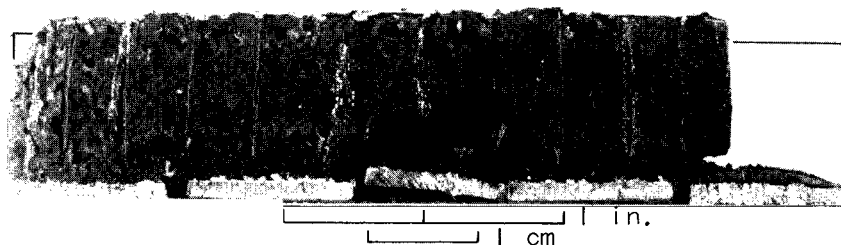
Figure 4.- Material E-3.



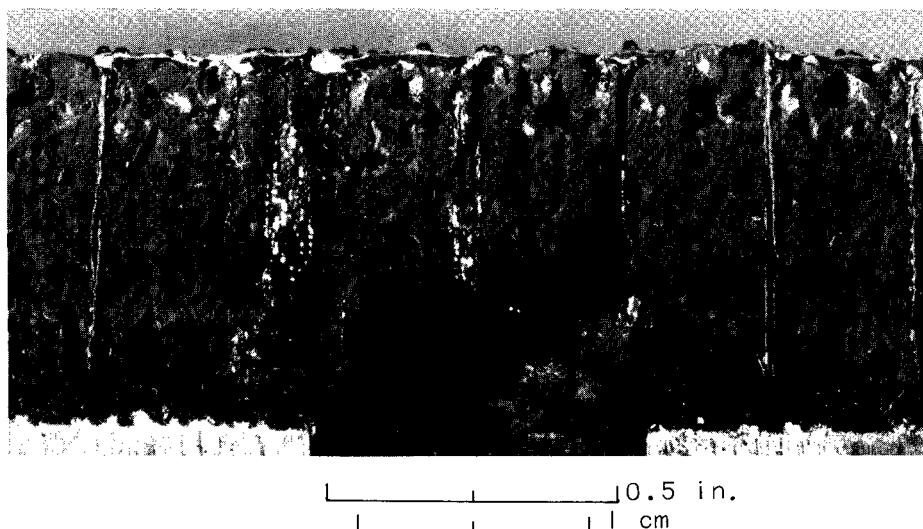
Front surface
before test



Front surface
after test



Sectioned specimen after test

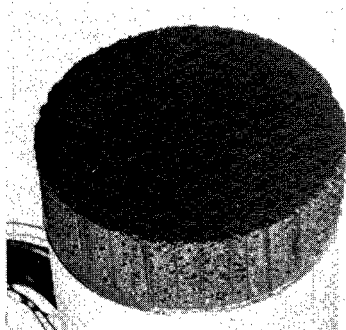


Sectioned specimen after test (enlarged view)

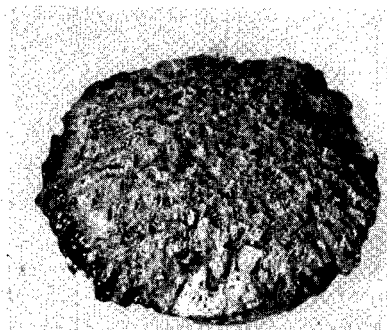
(b) Test condition B.

L-66-1154

Figure 4.- Continued.



Front surface
before test

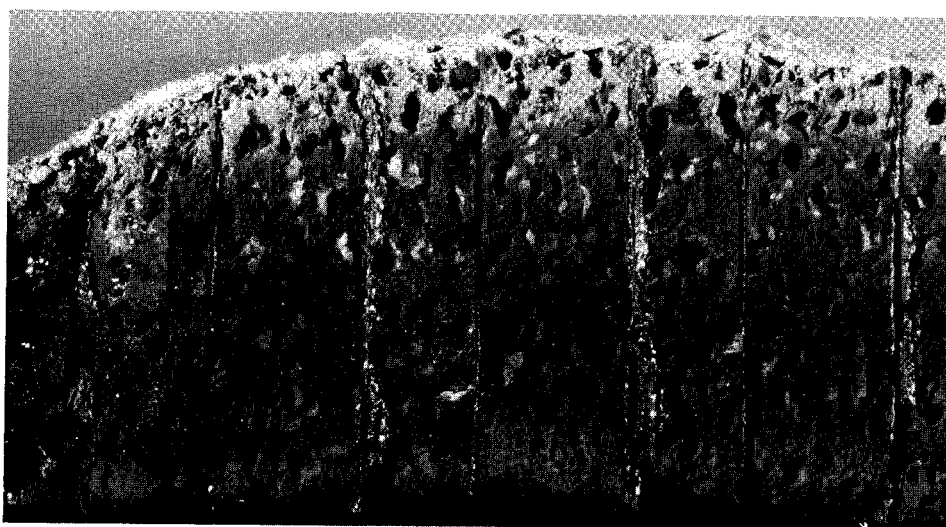


Front surface
after test



1 in.
1 cm

Sectioned specimen after test



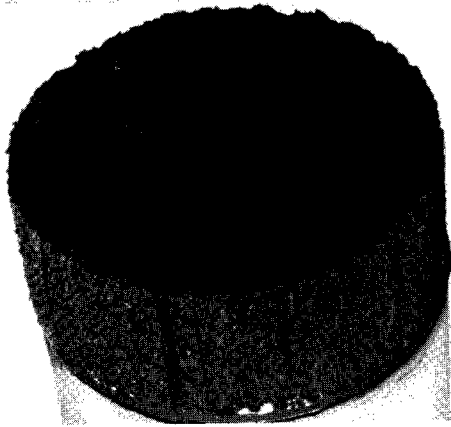
0.5 in.
1 cm

Sectioned specimen after test (enlarged view)

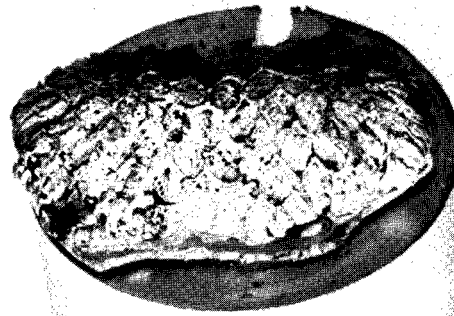
(c) Test condition C.

L-66-1155

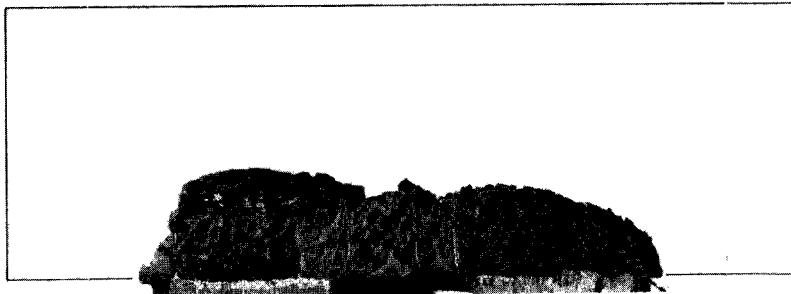
Figure 4.- Continued.



Front surface before test

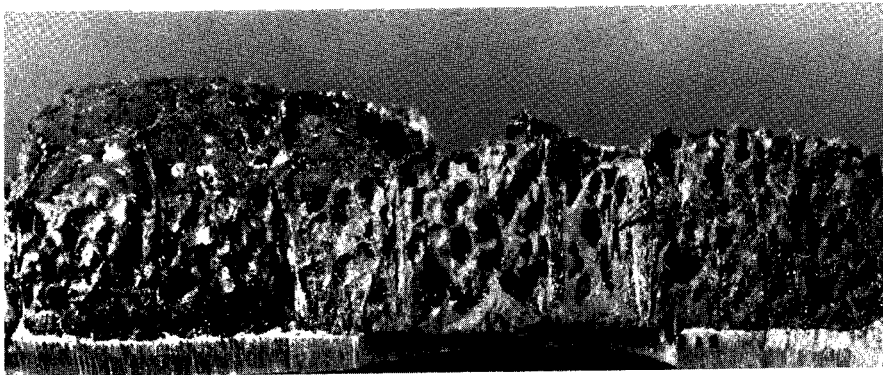


Front surface after test



1 in.
cm

Sectioned specimen after test



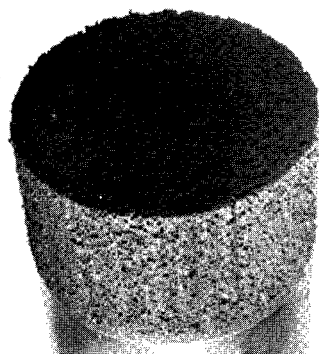
0.5 in.
cm

Sectioned specimen after test (enlarged view)

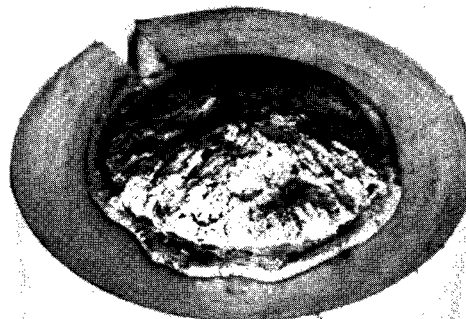
(d) Test condition D.

L-66-1156

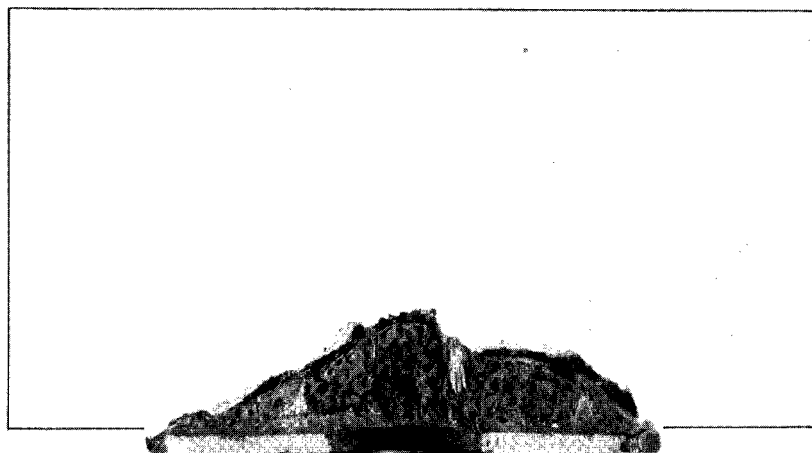
Figure 4.- Continued.



Front surface before test

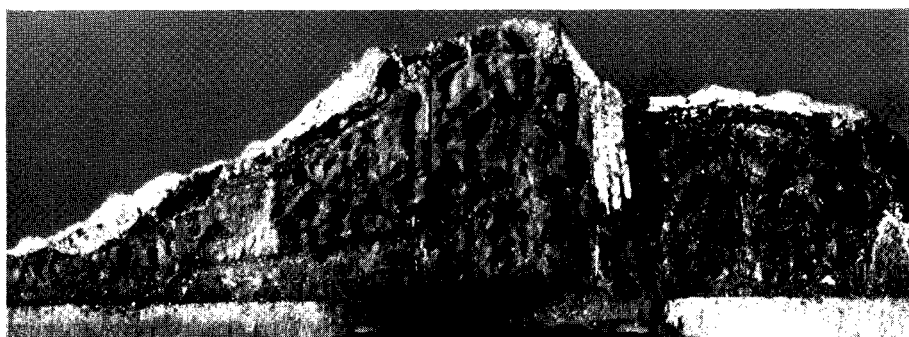


Front surface after test



1 in.
1 cm

Sectioned specimen after test



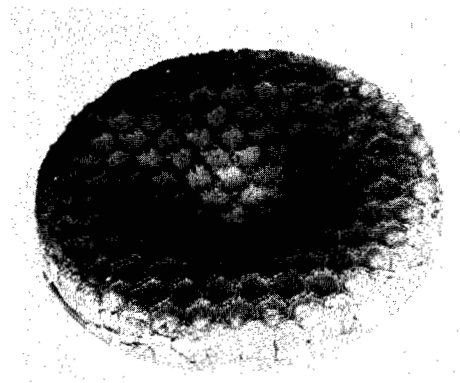
0.5 in.
1 cm

Sectioned specimen after test (enlarged view)

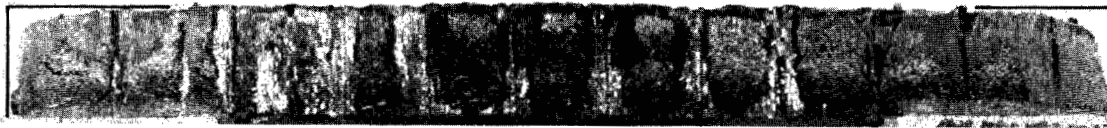
(e) Test condition E.

L-66-1157

Figure 4.- Concluded.



Front surface after test



1 in.
1 cm

Sectioned specimen after test



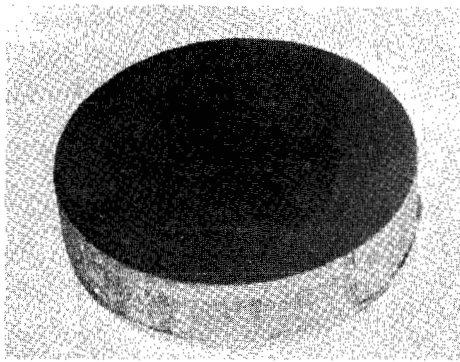
1 in.
1 cm

Sectioned specimen after test (enlarged view)

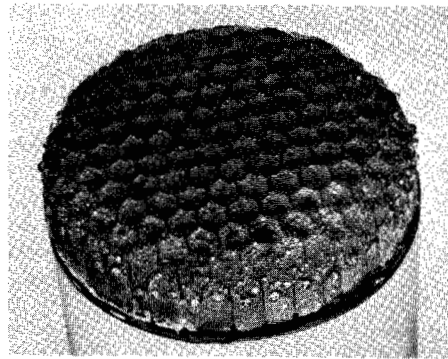
(a) Test condition A.

L-66-1158

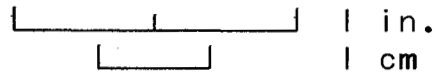
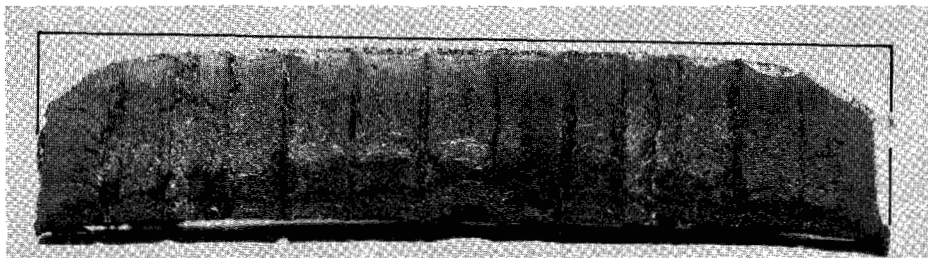
Figure 5.- Material R-1.



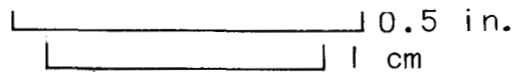
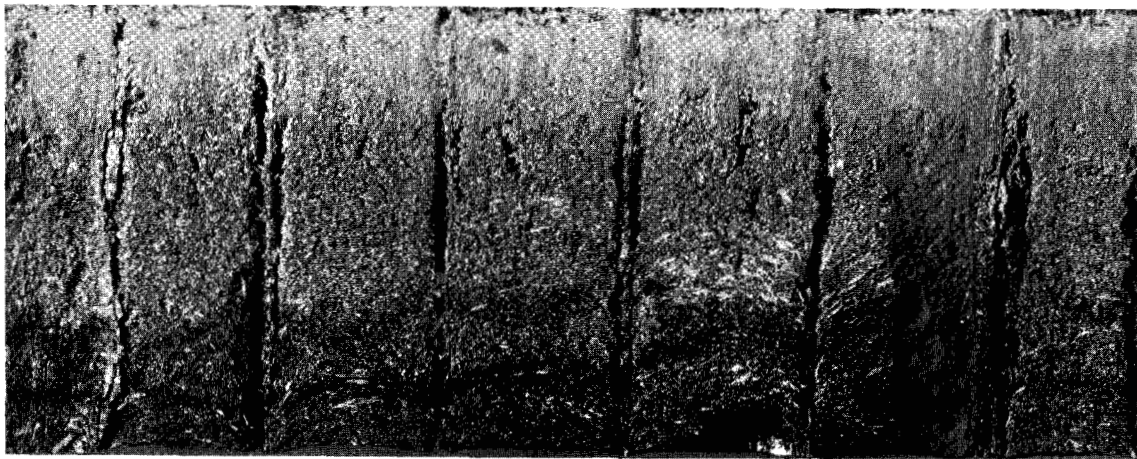
Front surface
before test



Front surface
after test



Sectioned specimen after test

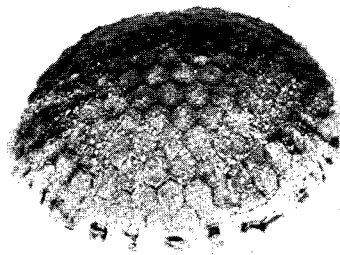
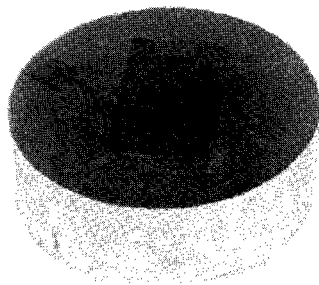


Sectioned specimen after test (enlarged view)

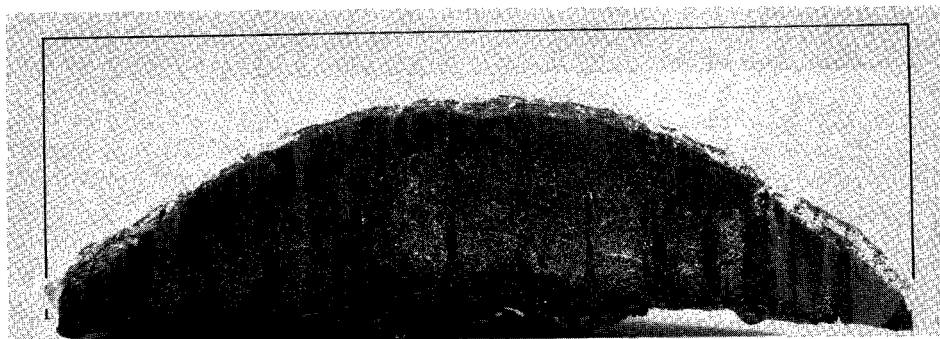
(b) Test condition B.

L-66-1159

Figure 5.- Continued.

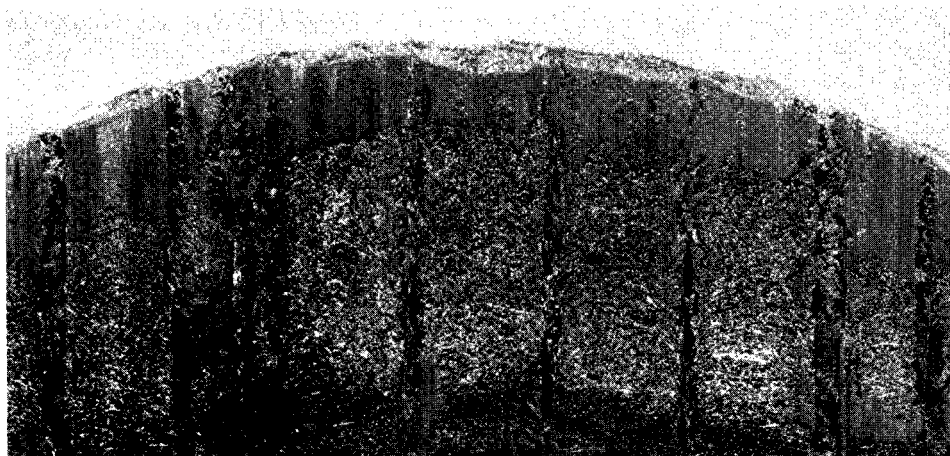


Front surface before test Front surface after test



1 in.
1 cm

Sectioned specimen after test



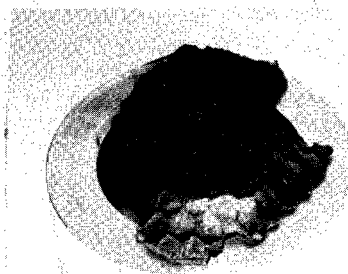
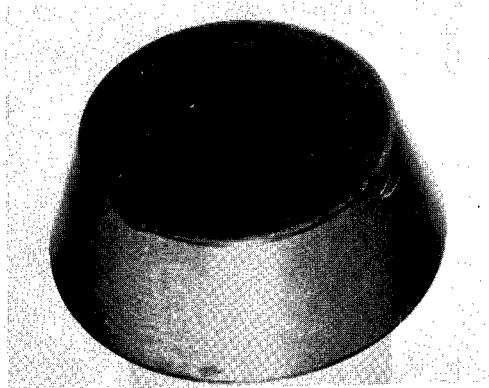
0.5 in.
1 cm

Sectioned specimen after test (enlarged view)

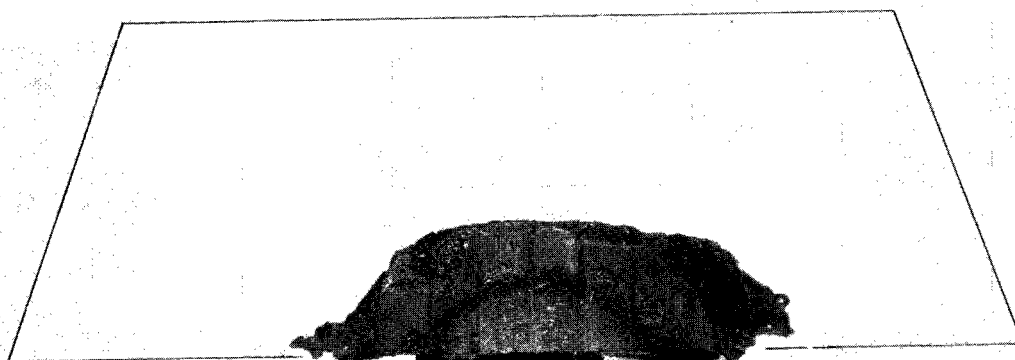
(c) Test condition C.

L-66-1160

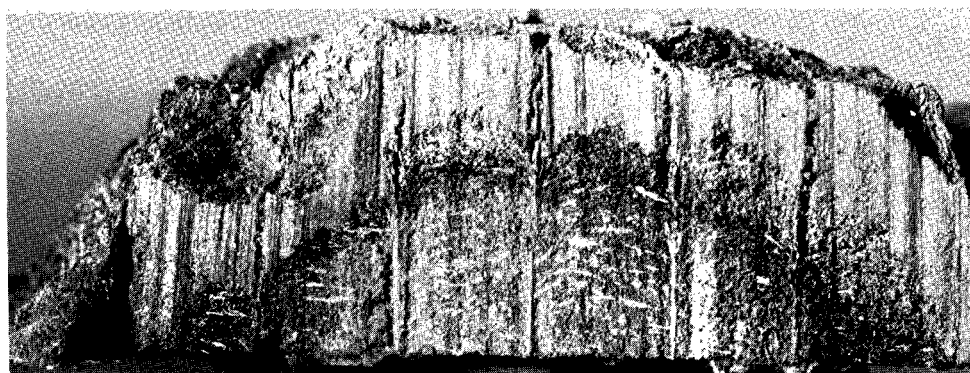
Figure 5.- Continued.



Front surface before test Front surface after test



Sectioned specimen after test

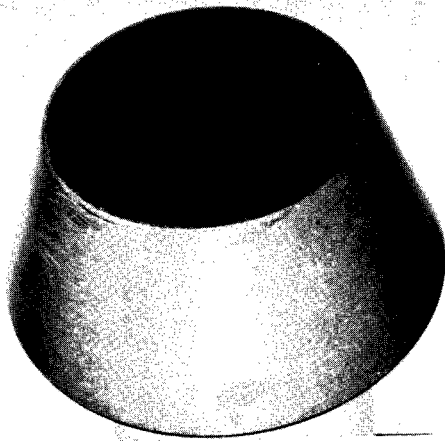


Sectioned specimen after test (enlarged view)

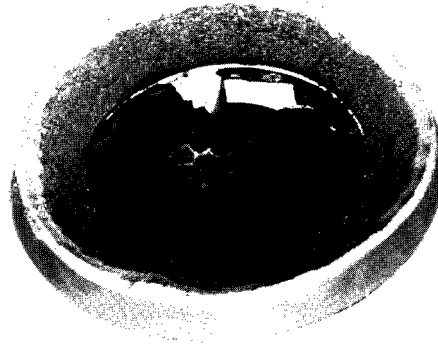
(d) Test condition D.

L-66-1161

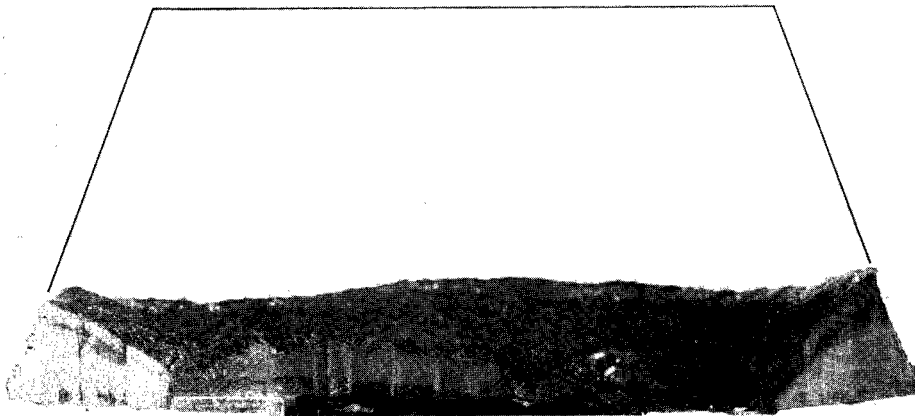
Figure 5.- Continued.



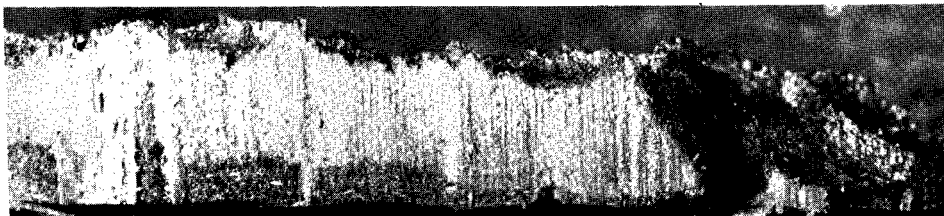
Front surface before test



Front surface after test



Sectioned specimen after test

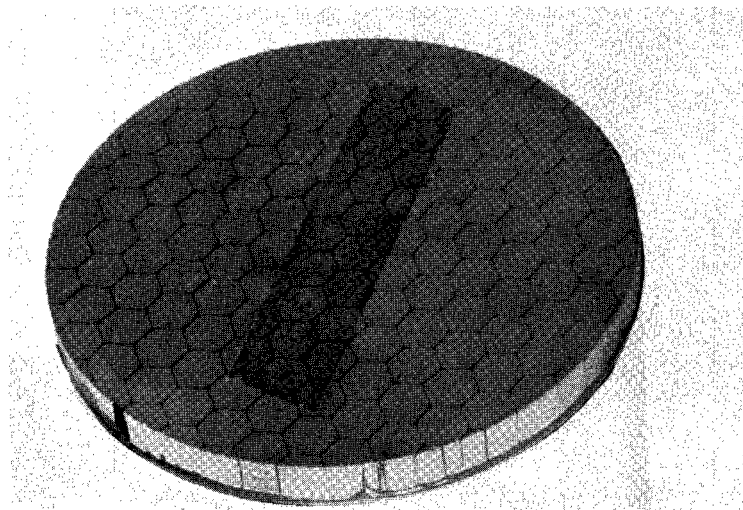



Sectioned specimen after test (enlarged view)

(e) Test condition E.

L-66-1162

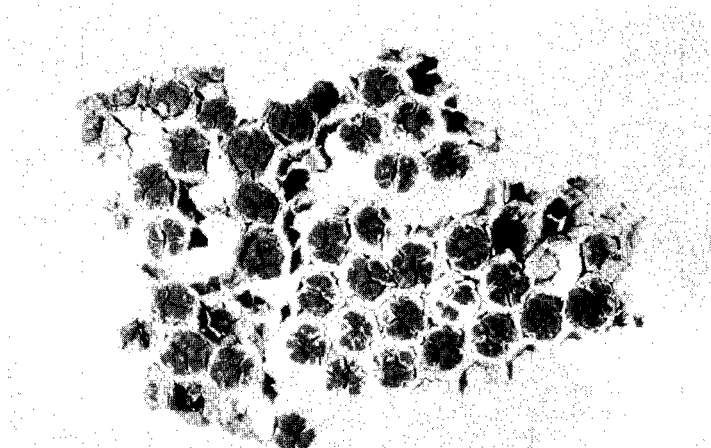
Figure 5.- Concluded.



1 in. 

1 cm 

Front surface before test



1 in. 

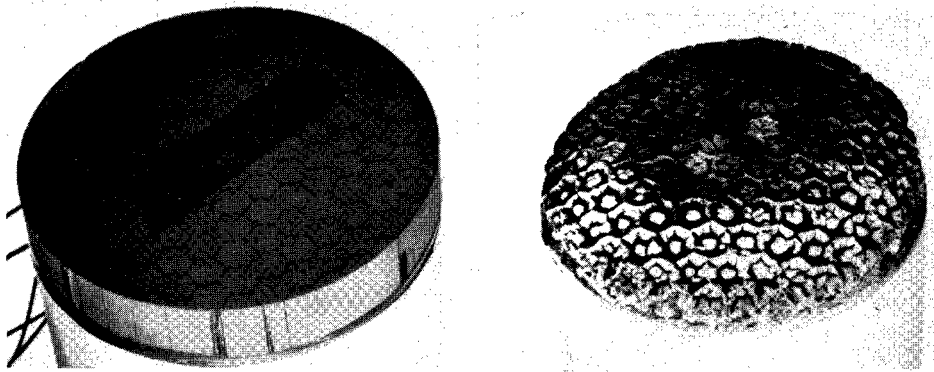
1 cm 

Front surface after test

(a) Test condition A.

L-66-1163

Figure 6.- Material R-2.

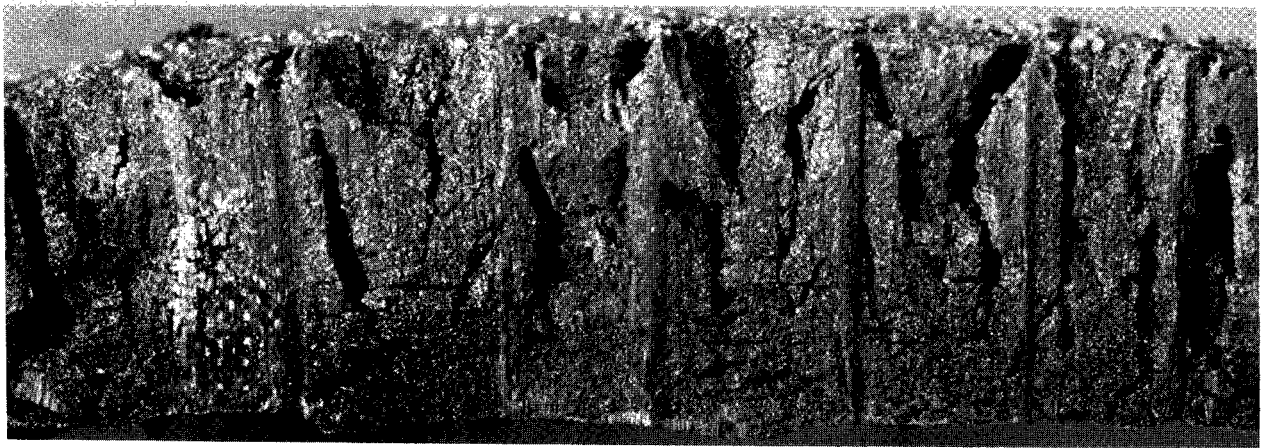


Front surface before test Front surface after test



1 in.
1 cm

Sectioned specimen after test



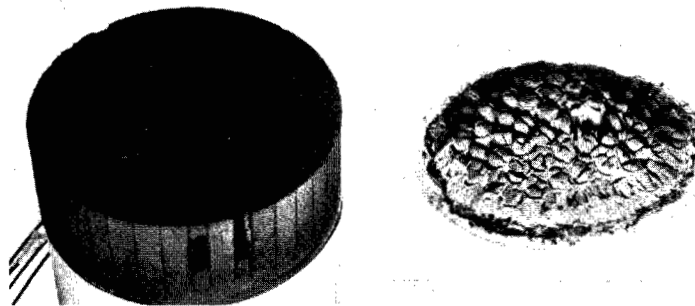
0.5 in.
1 cm

Sectioned specimen after test (enlarged view)

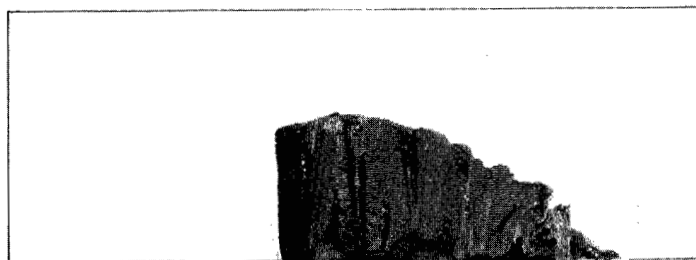
(b) Test condition B.

L-66-1164

Figure 6.- Continued.



Front surface before test Front surface after test



1 in.
1 cm

Sectioned specimen after test



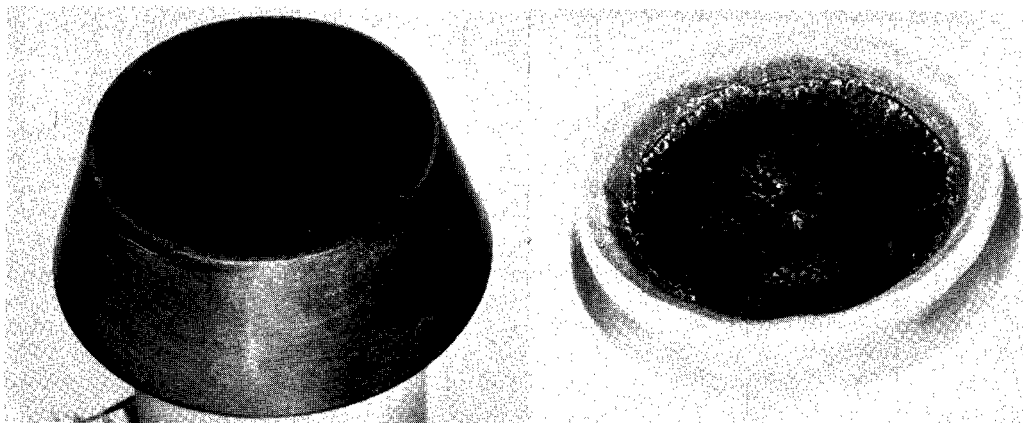
0.5 in. 1 cm

Sectioned specimen after test (enlarged view)

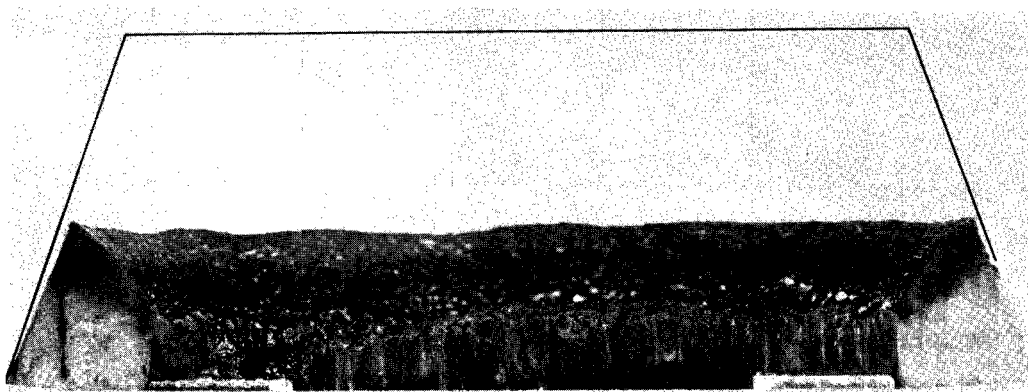
(c) Test condition C.

L-66-1165

Figure 6.- Continued.



Front surface before test Front surface after test



1 in.
1 cm

Sectioned specimen after test



0.5 in.
1 cm

Sectioned specimen after test (enlarged view)

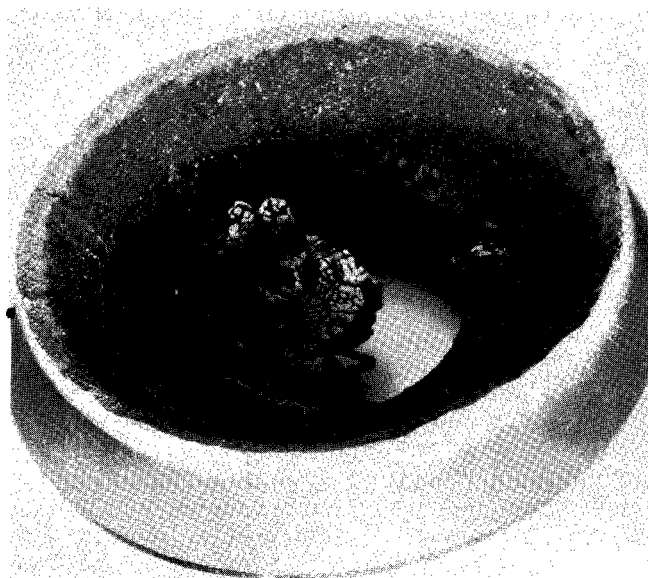
(d) Test condition D.



L-66-1166

Figure 6.- Continued.



Front surface before test

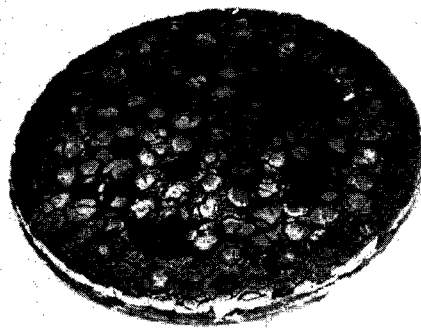


1 in. 
1 cm 
Front surface after test

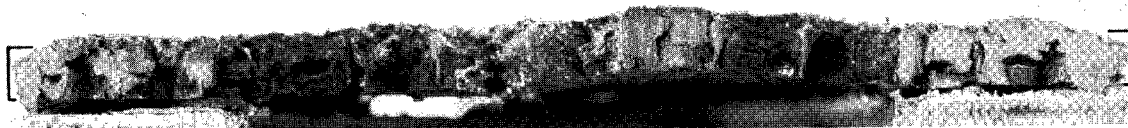
(e) Test condition E.

L-66-1167

Figure 6.- Concluded.

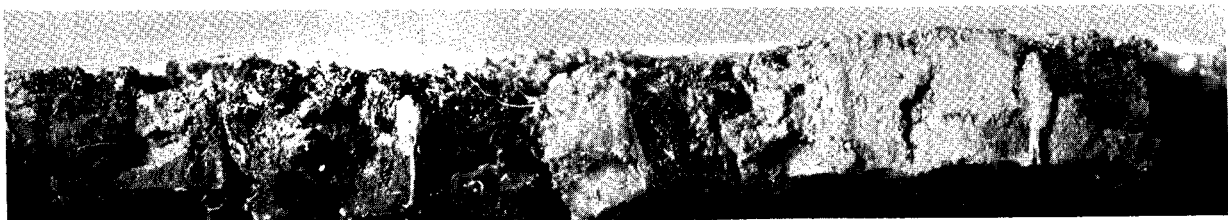


Front surface after test



1 in.
1 cm

Sectioned specimen after test



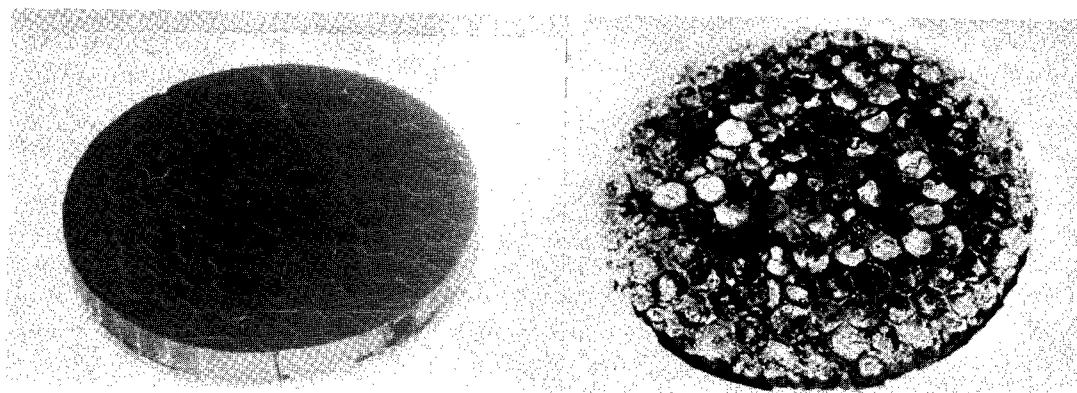
0.5 in.
1 cm

Sectioned specimen after test (enlarged view)

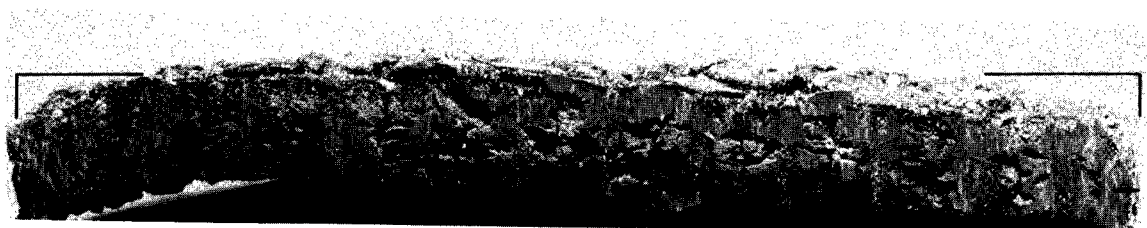
(a) Test condition A.

L-66-1168

Figure 7.- Material R-3.

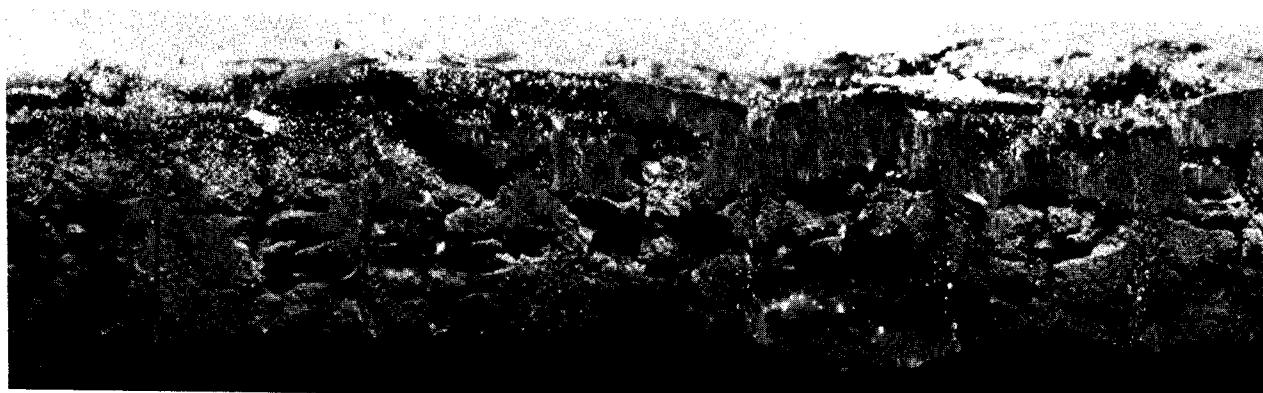


Front surface before test Front surface after test



1 in.
1 cm

Sectioned specimen after test



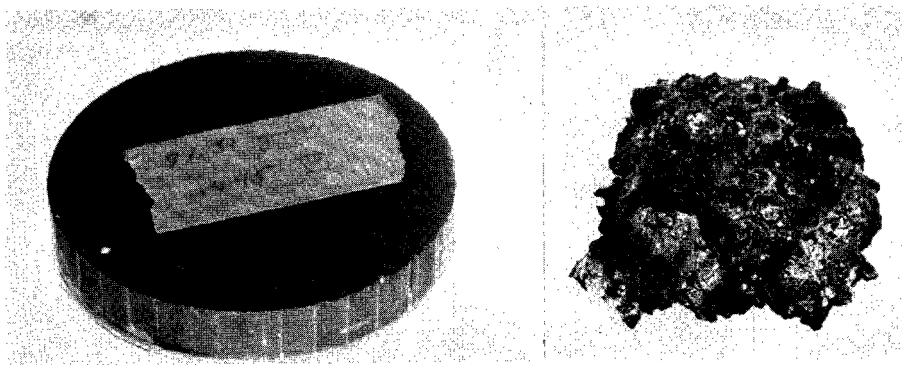
0.5 in.
1 cm

Sectioned specimen after test (enlarged view)

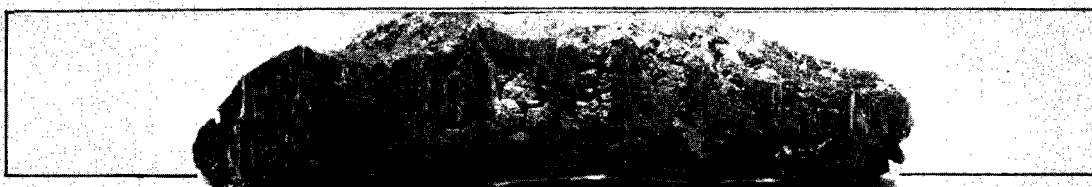
(b) Test condition B.

L-66-1169

Figure 7.- Continued.

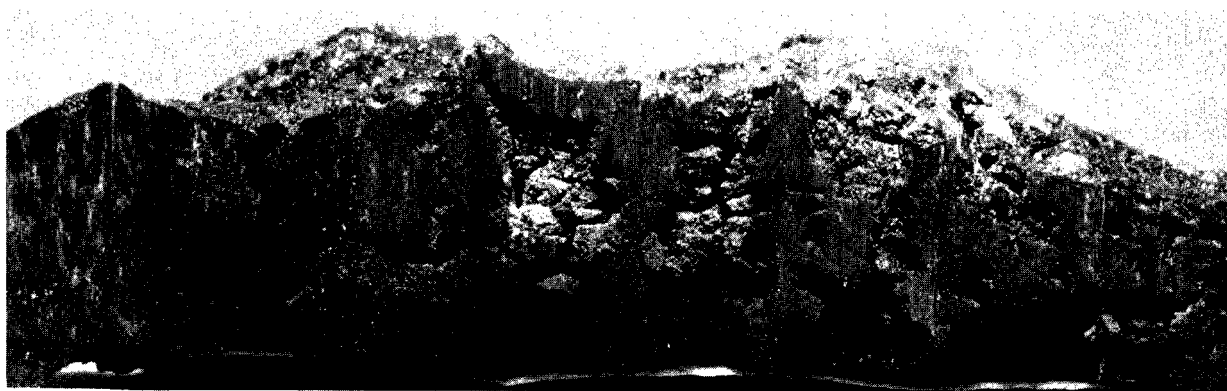


Front surface before test Front surface after test



1 in.
cm

Sectioned specimen after test



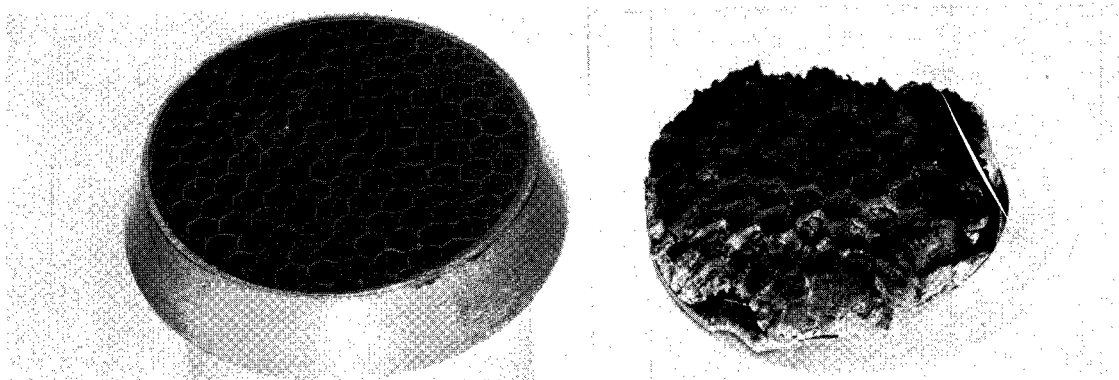
0.5 in.
cm

Sectioned specimen after test (enlarged view)

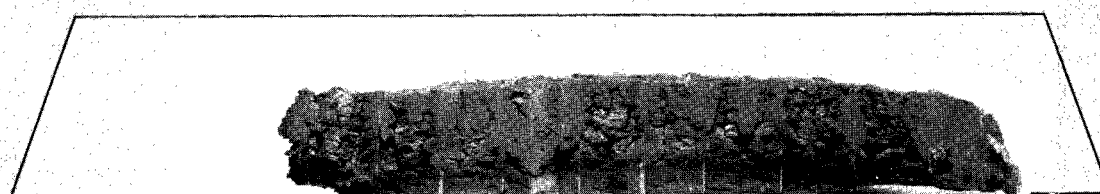
(c) Test condition C.

L-66-1170

Figure 7.- Continued.

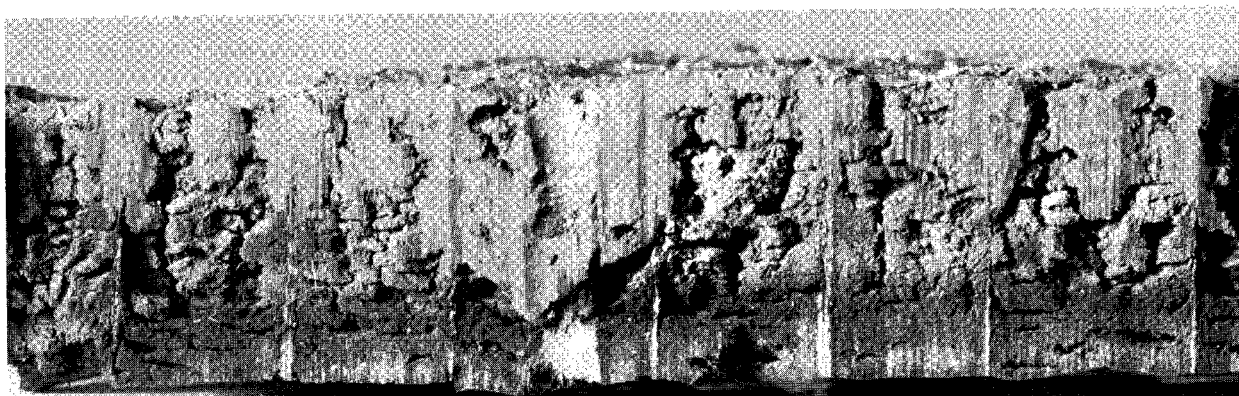


Front surface before test Front surface after test



1 in.
1 cm

Sectioned specimen after test



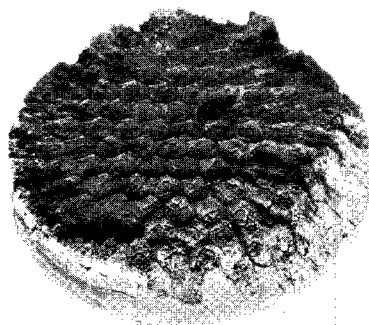
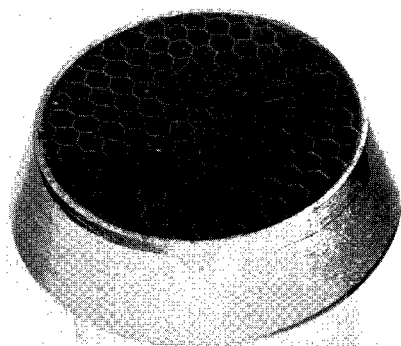
0.5 in.
1 cm

Sectioned specimen after test (enlarged view)

(d) Test condition D.

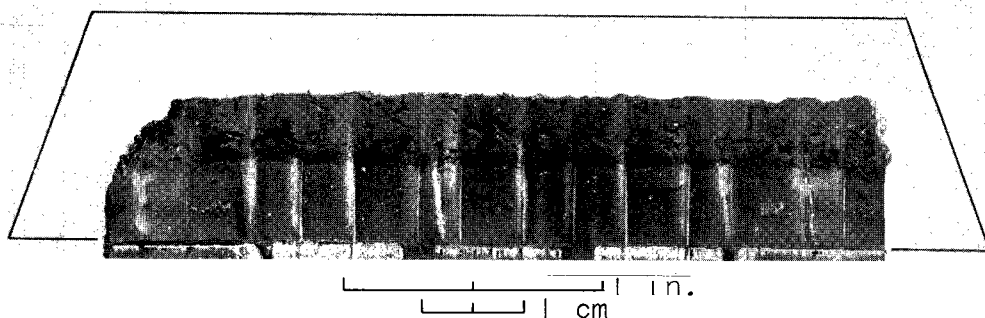
L-66-1171

Figure 7.- Continued.

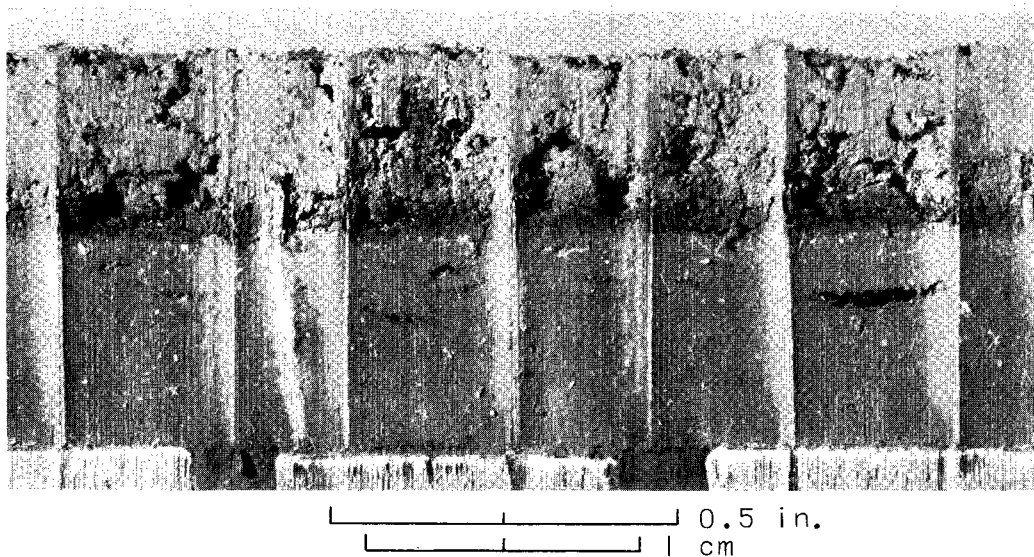


Front surface before test

Front surface after test



Sectioned specimen after test



Sectioned specimen after test (enlarged view)

(e) Test condition E.

L-66-1172

Figure 7.- Concluded.

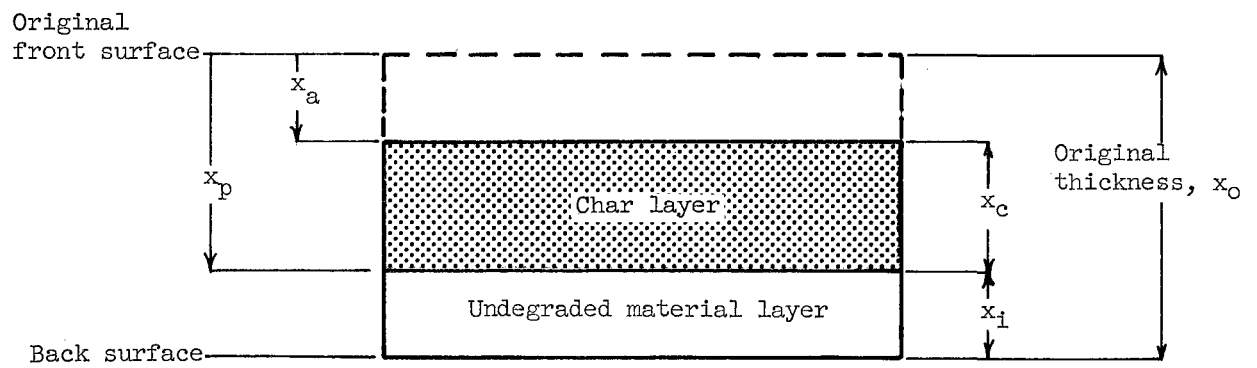
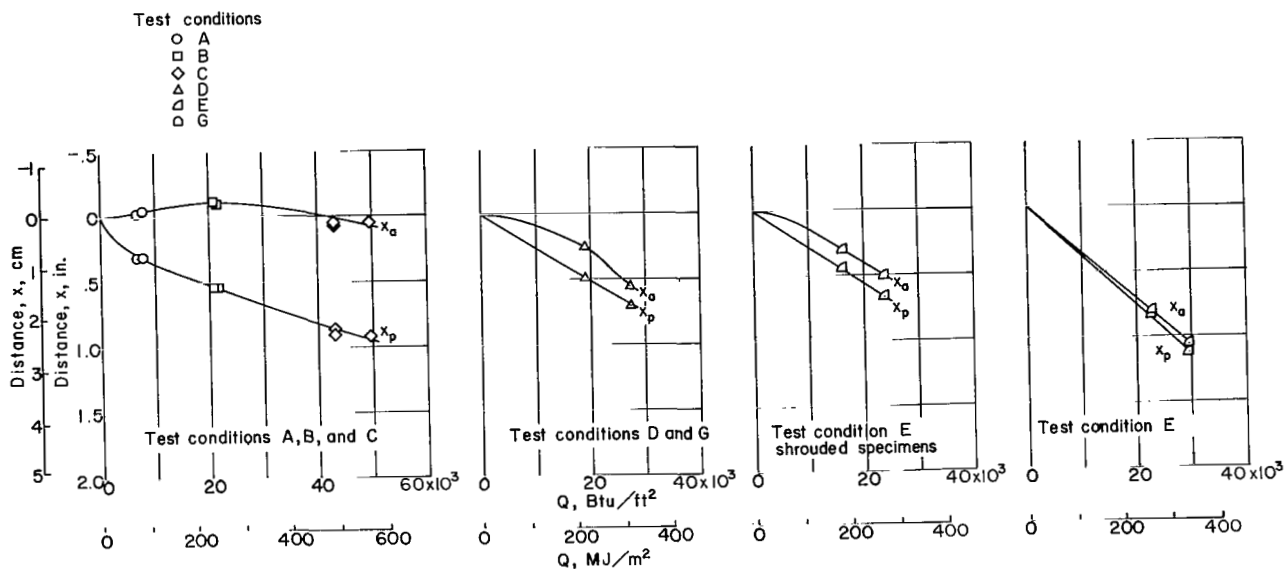
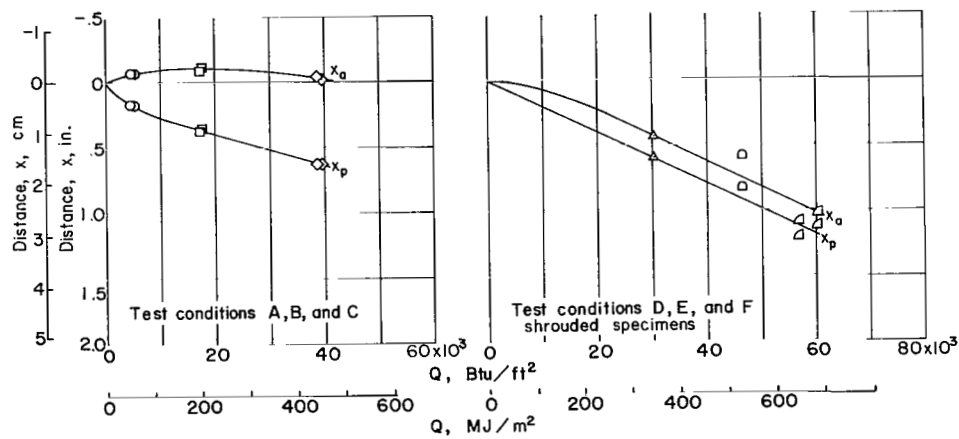


Figure 8.- Cross-section diagram and coordinate system for specimen dimensions.

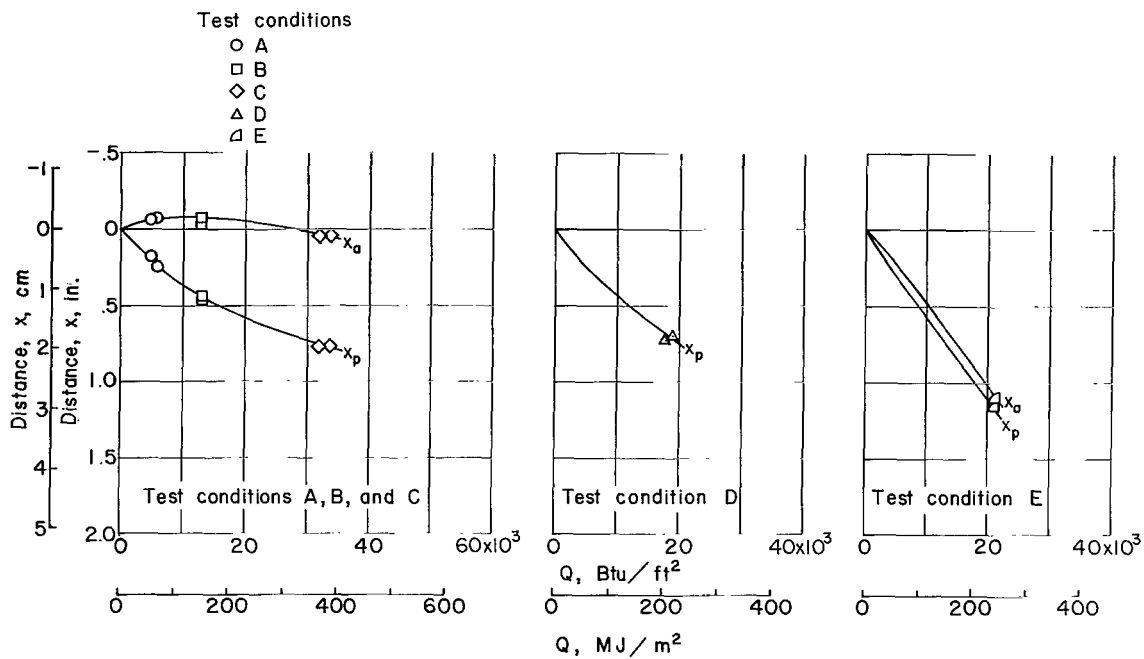


(a) Material E-1.

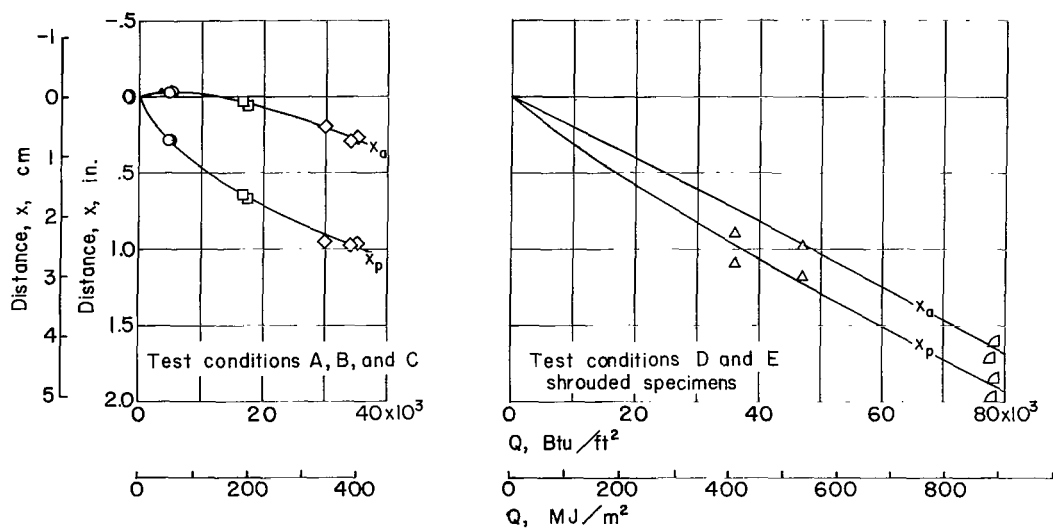


(b) Material E-2.

Figure 9.- Char surface and interface recessions as a function of cold-wall heat load.

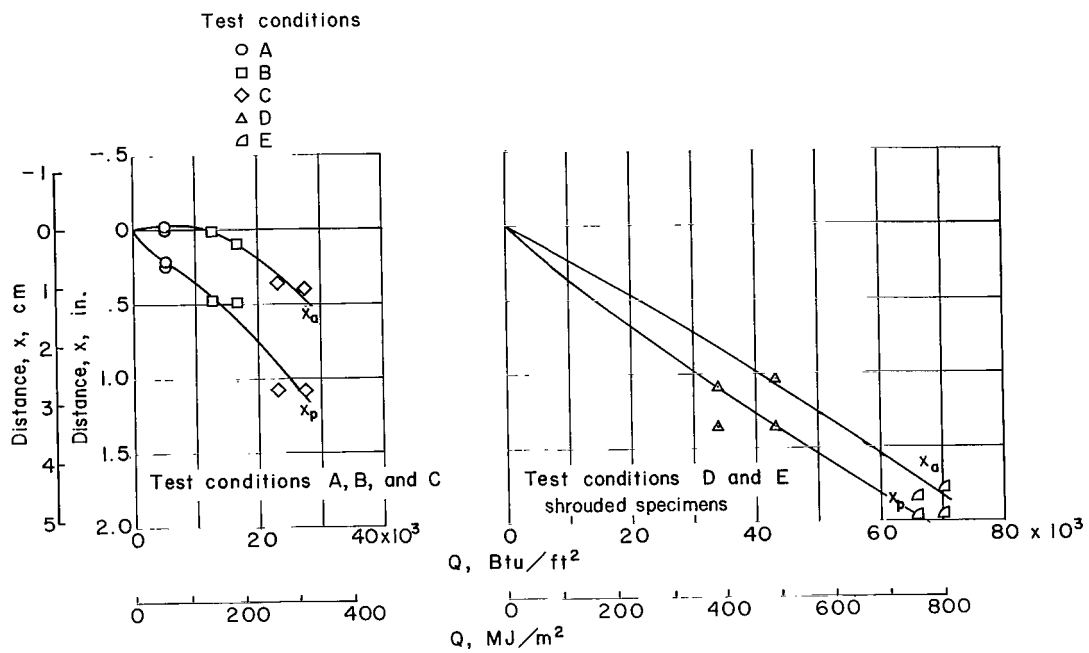


(c) Material E-3.

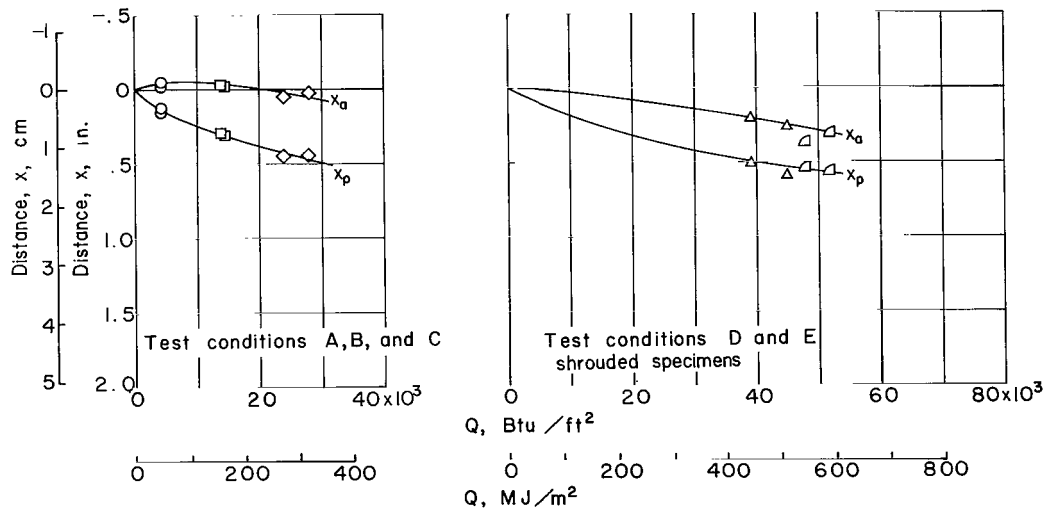


(d) Material R-1.

Figure 9.- Continued.



(e) Material R-2.



(f) Material R-3.

Figure 9.- Concluded.

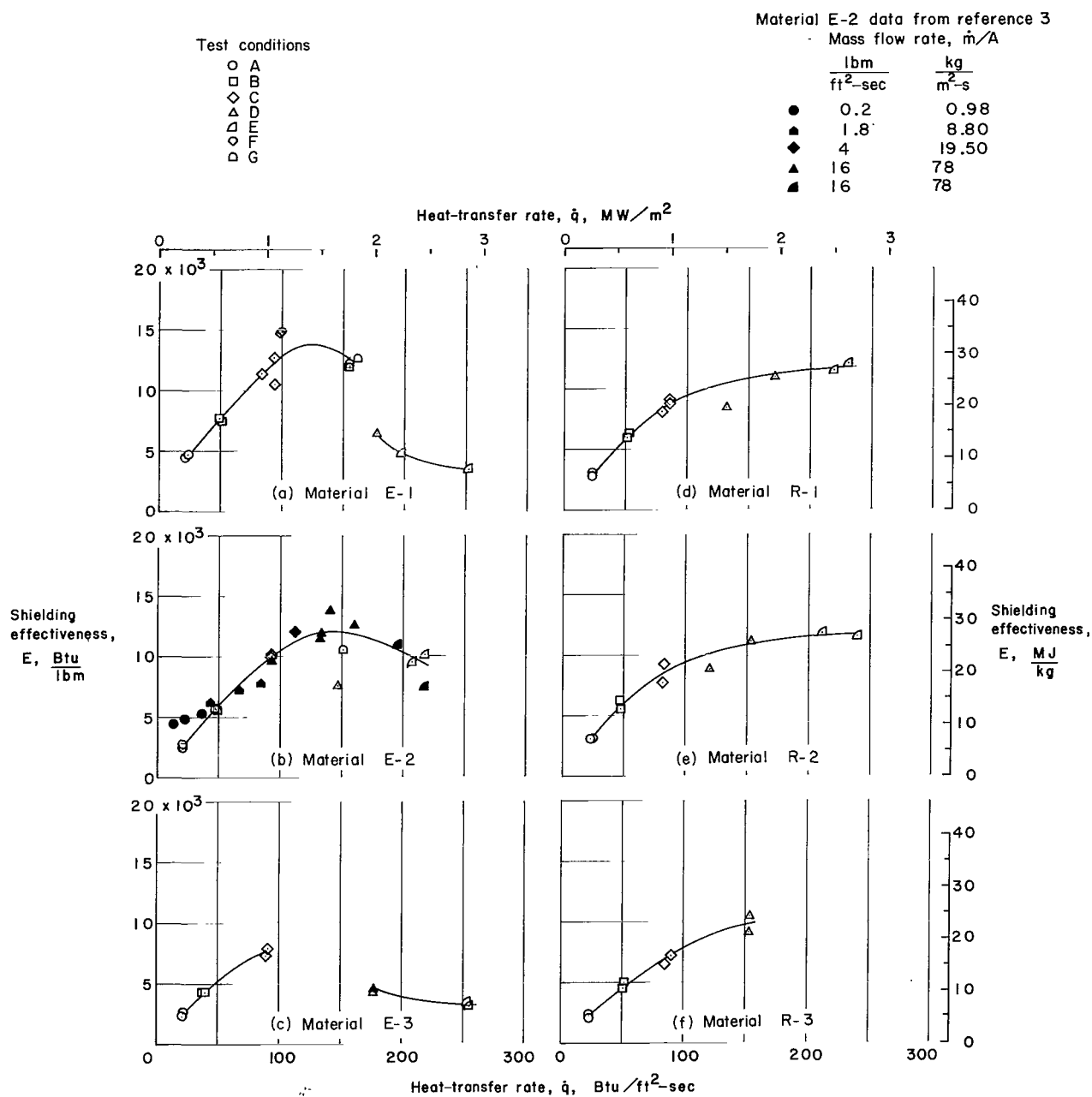


Figure 10.- Shielding effectiveness for a back-surface temperature rise of 300°F (167°K).

"The aeronautical and space activities of the United States shall be conducted so as to contribute . . . to the expansion of human knowledge of phenomena in the atmosphere and space. The Administration shall provide for the widest practicable and appropriate dissemination of information concerning its activities and the results thereof."

—NATIONAL AERONAUTICS AND SPACE ACT OF 1958

NASA SCIENTIFIC AND TECHNICAL PUBLICATIONS

TECHNICAL REPORTS: Scientific and technical information considered important, complete, and a lasting contribution to existing knowledge.

TECHNICAL NOTES: Information less broad in scope but nevertheless of importance as a contribution to existing knowledge.

TECHNICAL MEMORANDUMS: Information receiving limited distribution because of preliminary data, security classification, or other reasons.

CONTRACTOR REPORTS: Technical information generated in connection with a NASA contract or grant and released under NASA auspices.

TECHNICAL TRANSLATIONS: Information published in a foreign language considered to merit NASA distribution in English.

TECHNICAL REPRINTS: Information derived from NASA activities and initially published in the form of journal articles.

SPECIAL PUBLICATIONS: Information derived from or of value to NASA activities but not necessarily reporting the results of individual NASA-programmed scientific efforts. Publications include conference proceedings, monographs, data compilations, handbooks, sourcebooks, and special bibliographies.

Details on the availability of these publications may be obtained from:

SCIENTIFIC AND TECHNICAL INFORMATION DIVISION
NATIONAL AERONAUTICS AND SPACE ADMINISTRATION
Washington, D.C. 20546